NRC Research Press

ARTICLE

Calibration of the zooplankton community size spectrum as an indicator of change in Canadian Shield lakes

Lauren Emily Barth, Brian John Shuter, William Gary Sprules, Charles Kenneth Minns, and James Anthony Rusak

Abstract: Developing the crustacean zooplankton community size spectrum into an indicator of change in lakes requires quantification of the natural variability in the size spectrum related to broad-scale seasonal, annual, and spatial factors. Characterizing seasonal patterns of variation in the size spectrum is necessary so that monitoring programs can be designed to minimize the masking effects that seasonal processes can have on detecting longer-term temporal change. We used a random effects model to measure monthly, annual, and interlake variability in the slope (i.e., relative abundance of small and large organisms) and centered height (i.e., total abundance) of the crustacean zooplankton normalized abundance size spectrum from 1981 to 2011 among eight Canadian Shield lakes. Consistent with theoretical predictions, the slope was a relatively stable characteristic of the zooplankton community compared with the height, which varied significantly among lakes. We identified a seasonal signal in height and slope and used a mixed effects model to characterize the linear rate of change from May to October; there was an overall decline in height and an overall increase in slope. Seasonal variance was greater than annual variance for both the height and the slope, suggesting that long-term monitoring of lakes and interlake comparisons using zooplankton size spectra should be based on temporally standardized sampling protocols that minimize the effects of seasonal processes. We recommend sampling the zooplankton community in midsummer because this results in size spectrum estimates close to seasonal mean values.

Résumé : L'utilisation du spectre de tailles de communautés de zooplancton crustacé comme indicateur de changement dans les lacs nécessite la quantification de la variabilité naturelle dans le spectre de tailles associée à des facteurs saisonniers, annuels et spatiaux à grande échelle. La caractérisation des motifs saisonniers de variation dans le spectre de tailles est nécessaire pour concevoir des programmes de surveillance qui minimisent les effets de masquage que peuvent exercer des processus saisonniers sur la détection de changements à long terme. Nous avons utilisé un modèle d'effets aléatoires pour mesurer la variabilité mensuelle, annuelle et entre lacs de la pente (c.-à-d. l'abondance relative des organismes de petite et grande taille) et la hauteur centrée (c.-à-d. l'abondance totale) du spectre d'abondance selon la taille normalisé de zooplancton crustacé de 1981 à 2011 pour huit lacs du Bouclier canadien. Conformément aux prédictions théoriques, la pente s'avère une caractéristique relativement stable de la communauté de zooplancton comparativement à la hauteur, qui varie significativement entre les lacs. Nous relevons un signal saisonnier dans la hauteur et la pente et utilisons un modèle à effets mixtes pour caractériser le taux linéaire de changement de mai à octobre; il en ressort une baisse globale de la hauteur et une hausse globale de la pente. La variance saisonnière est plus grande que la variance annuelle tant pour la hauteur que pour la pente, donnant à penser que la surveillance à long terme de lacs et les comparaisons entre lacs qui font appel aux spectres de tailles du zooplancton devraient reposer sur des protocoles d'échantillonnage à normalisation temporelle qui minimisent les effets de processus saisonniers. Nous recommandons l'échantillonnage des communautés de zooplancton au milieu de l'été puisque cela produit des estimations du spectre de tailles s'approchant des valeurs moyennes saisonnières. [Traduit par la Rédaction]

Introduction

Many indicators have been developed to provide information about the composition, structure, or function of aquatic ecosystems (Great Lakes Water Quality and Science Advisory Boards 2013). However, a key challenge has been to identify a set of indicators that are simple to implement, easy to interpret, and provide useful information about the state of these systems. The International Joint Commission (2014) identified a small number of ecosystem indicators for the Great Lakes basin ecosystem that includes physical (e.g., water level and temperature), chemical (e.g., phosphorus), and biological (e.g., aquatic invasive species and harmful, nuisance algae) indicators. Lower food web productivity and health were regarded as core indicators that focus on the efficiency of energy transfer from phytoplankton to fish. Thus, simple food web metrics of lower trophic levels may provide valuable tools for monitoring the condition of lakes over the long term.

Zooplankton are an integral part of aquatic systems, providing the bridge between phytoplankton primary production and fish.

Received 24 September 2018. Accepted 19 March 2019.

L.E. Barth. Department of Biology, University of Toronto Mississauga, Mississauga, ON L5L 1C6, Canada; Department of Ecology and Evolutionary Biology, University of Toronto, 25 Willcocks Street, Toronto, Ontario, ON M5S 3B2, Canada.
B.J. Shuter and C.K. Minns. Department of Ecology and Evolutionary Biology, University of Toronto, 25 Willcocks Street, Toronto, Ontario, ON M5S 3B2, Canada.
W.G. Sprules. Department of Biology, University of Toronto Mississauga, Mississauga, ON L5L 1C6, Canada.
J.A. Rusak. Dorset Environmental Science Centre, Ontario Ministry of Environment and Climate Change, 1026 Bellwood Acres Road, P.O. Box 39, Dorset, ON P0A 1E0, Canada.

Corresponding author: Lauren Emily Barth (email: lauren.barth@mail.utoronto.ca).

Zooplankton communities are sensitive to changes in both their prey source and their predators, reflecting a balance of food web processes in their size and taxonomic composition (Mills and Schiavone 1982; Hansson et al. 2007). Their taxonomic composition, production, and average body size have been shown to be sensitive indicators of lake trophy (Jeppesen et al. 2000), the introduction of non-native invasive species (Yan et al. 2001), acidification (Jeziorski et al. 2008), and climate features (Richardson 2018). Accordingly, zooplankton community metrics offer a promising avenue for the development of indicators of perturbation in both top-down and bottom-up processes.

The body size of individuals is a relatively simple metric to obtain, and it is a fundamental trait that is correlated with many physiological and ecological phenomena. The size of an individual scales with variables such as its metabolic rate, life history characteristics, diet breadth, mortality rate, somatic and population growth rates, and trophic position (Peters 1983; Cohen et al. 1993; Jennings et al. 2001). The usefulness of body size indicators to monitor fish communities (e.g., the large fish indicator; Modica et al. 2014) and detect alterations in food web structure (e.g., mean body size of zooplankton; Gorokhova et al. 2016) is well known. However, zooplankton size-based indicators tend to be coarse-scale metrics of mean body size of the community (Xu et al. 2001) or taxonomic group (e.g., cladocerans; Yan et al. 2008), and focusing solely on mean body size can obscure important information about the structure and functioning of these size-structured food webs.

The size spectrum, first introduced by Sheldon and Parsons (1967) to describe the distribution of organism abundance or biomass as it relates to body size, has become an important tool for understanding size-structured communities. This method involves grouping individuals into logarithmically equal size bins irrespective of their taxonomy (Blanco et al. 1994). The primary structure of the size spectrum typically follows a log–log relationship between abundance (or normalized biomass) and body size that is linear with a slope of approximately –1 — a pattern that is consistent with a steady state condition of roughly equal biomass within logarithmically equal size bins (Sprules and Barth 2016). This relationship reflects energy losses through food webs due to size-dependent metabolic and predation rates (Rossberg 2012). Primary production in pelagic systems is dominated by single-celled algae with high population growth rates (McGarvey et al. 2016). Herbivores and predators typically increase in size at each step up in trophic level (Jennings et al. 2001), but energy is lost due to individual feeding and metabolic costs at each of these energy transfer points (Peters 1983). This translates into less energy available to higher trophic levels. These energetic and ecological allometric relationships help explain the universal observation that small individuals are more abundant than large ones in aquatic ecosystems. Thus, the size spectrum of a community represents a "basic underlying ecosystem condition or pattern" that is constrained by the physiological and ecological limits that all individuals within an aquatic ecosystem share (Gamble et al. 2006; Sprules 2008).

The ubiquity of a spectral slope of –1, observed in a wide range of ecosystems (Sprules and Barth 2016), spurred interest in examining whether the primary structure of the size spectrum could be used to identify a perturbation that has shifted the size spectrum away from its steady-state condition. The use of a linear model to characterize the size spectrum simplifies this type of analysis to assessing change in just two easily interpretable parameters — the slope of the line and its height (i.e., the abundance at the center of the size spectrum): the height reflects the overall abundance of organisms in the community, while the slope reflects the relative abundance of small and large organisms (Ahrens and Peters 1991). Empirical size spectra have been used extensively as indicators of exploited fish communities because fishing practices are generally size-selective, targeting the largest fish, which changes the slope of the fish community size spectrum (Blanchard et al. 2005; Emmrich et al. 2011; McCann et al. 2016). However, there is mixed evidence about whether the size spectrum of lower trophic levels or complete pelagic communities can be used as indicators of perturbation. There is empirical evidence supporting the notion that size spectral slopes are constant, with height varying systematically with lake characteristics (Boudreau and Dickie 1992; Gamble et al. 2006; Sprules 2008). On the other hand, there is also a body of evidence suggesting that the slope varies systematically with lake characteristics (Sprules and Munawar 1986; Ahrens and Peters 1991; Moore and Suthers 2006). Hence, there is a need to characterize the natural variability in the size spectrum of lower trophic levels before it can be developed into a tool to monitor aquatic ecosystems.

In this paper we test the utility of the zooplankton size spectrum as an indicator of ecosystem change using a long-term data set on zooplankton communities in lakes from south-central Ontario that vary in environmental and ecological characteristics through time and among lakes (Molot and Dillon 2008; Yan et al. 2008; Yao et al. 2013). We measure the relative variance in the slope and the height of the zooplankton normalized abundance size spectrum (NASS) associated with temporal (months and years) and spatial (among lakes) variability in the data set. We expect that parameters of the zooplankton size spectrum will be most strongly associated with spatial variability, as others have found for zooplankton communities (Kratz et al. 1987; Patalas 1990; Rusak et al. 2002), but that the slope of the size spectrum will be more conserved than the height given the relatively narrow range of parameter values governing size-dependent ecological processes that structure energy flow in aquatic communities (Boudreau and Dickie 1992; Sprules 2008). We also expect the community size spectrum to reflect typical seasonal patterns in zooplankton with greater slopes and heights in the spring, caused by high abundance of smaller species, to shallower slopes and reduced heights in the summer, reflecting greater abundances of larger species (Sommer et al. 1986).

A second objective of our study was to identify the optimal time of year to sample zooplankton — when the zooplankton NASS parameters deviated the least from their seasonal average — by determining the magnitude and consistency, across years and lakes, of seasonal patterns in the height and slope of the zooplankton NASS. We aim to evaluate the sensitivity of the zooplankton size spectrum to ecological changes and make recommendations about methodological considerations for long-term monitoring programs using zooplankton community size spectra.

Methods

The study lakes

The eight Dorset Environmental Science Centre (DESC) long-term study lakes are similar to one another in many limnological characteristics (Table 1). They are small (<100 ha), nutrient-poor lakes in forested watersheds located in the Haliburton–Muskoka region on the southern edge of the Precambrian Shield in central Ontario, Canada (Fig. 1) (Rusak et al. 1999; Molot and Dillon 2008). Six of these lakes are dimictic and become strongly stratified by July, whereas Dickie Lake stratifies weakly and Heney Lake does not stratify at all (Table 1) (Rusak et al. 1999). There are many important differences among these lakes. For example, the abundance of the most dominant macroinvertebrate predator in temperate lakes, (i.e., *Chaoborus*, the phantom midge) varies widely (Table 1; Pawson and McEachern 1987). These lakes vary greatly in their sensitivity to acid deposition and to total phosphorus (TP) load attributable to shoreline development. Both Blue Chalk and Red Chalk Lake are reference systems because they are clear, dimictic lakes that have been unaffected by shoreline development, acid rain, or invasive zooplanktivores (Yan et al. 2008).

Table 1. Physical, chemical, and biological attributes of the eight Dorset Environmental Science Centre (DESC) study lakes.

Lake	Lat. (N)	Long. (W)	A_o	z_{max}	z_{mean}	Secchi	TP	DOC	pH	Strat.	Stress	*Chaob.*
BC	45°12′	78°56′	52.4	23.0	8.5	6.8	4.24	2.26	7.02	S		8.0
CB	45°13′	78°59′	34.4	27.0	8.9	3.0	5.40	6.66	6.25	S	A	133.2
CN	45°05′	79°02′	56.7	25.0	9.2	3.3	6.55	5.46	6.19	S	A	8.6
DE	45°09′	79°05′	93.6	12.0	5.0	2.9	8.06	6.37	6.58	W	A, P	65.1
HP	45°23′	79°07′	71.4	37.5	13.3	4.5	4.82	4.66	6.85	S	P, NIS	0.1
HY	45°08′	79°06′	21.4	5.8	3.3	4.3	6.22	4.01	6.07	A	A	0.3
PC	45°11′	78°50′	32.1	16.3	7.9	7.7	3.40	2.51	6.03	S	A	58.8
RCM	45°11′	78°56′	44.1	38.0	16.7	5.6	3.90	3.39	6.89	S		0.2

Note: Lake abbreviations: Blue Chalk (BC), Chub (CB), Crosson (CN), Dickie (DE), Harp (HP), Heney (HY), Plastic (PC), and Red Chalk–main basin (RCM). Geographic and morphometric characteristics (surface area (A_o, ha), maximum depth (z_{max}, m), and mean depth (z_{mean}, m)) are from Rusak et al. (1999). Secchi depth (Secchi, m), total phosphorus (TP, μg·L^{-1}), and dissolved organic carbon (DOC, mg·L^{-1}) are mean values calculated over biweekly to monthly collected data in June–August of 2005–2009 (provided by J. Rusak, Ontario Ministry of Environment and Climate Change, unpublished data, 2018). Strength of summer stratification (Strat.: strong (S), weak (W), or normally absent (A)) and lake stress (Stress: acidification (A), high phosphorus loading from shoreline development (P), and introduction of nonindigenous species (NIS)) are from Yan et al. (2008). *Chaoborus* abundance (*Chaob.*: no.·m^{-3}) represents the mean concentration, weighted by lake area and volume, from ten stations sampled in fall (from Pawson and McEachern 1987).

Fig. 1. Locations of the Dorset study lakes in central Ontario, Canada, in reference to main roads and the Dorset Environmental Science Centre (geospatial data sources: Great Lakes Information Network (GLIN), hydroLAKES database (Messager et al. 2016), CanMap RoutLogistics Ontario by DMTI Spatial Inc., 2011, and ESRI Inc., 2012).

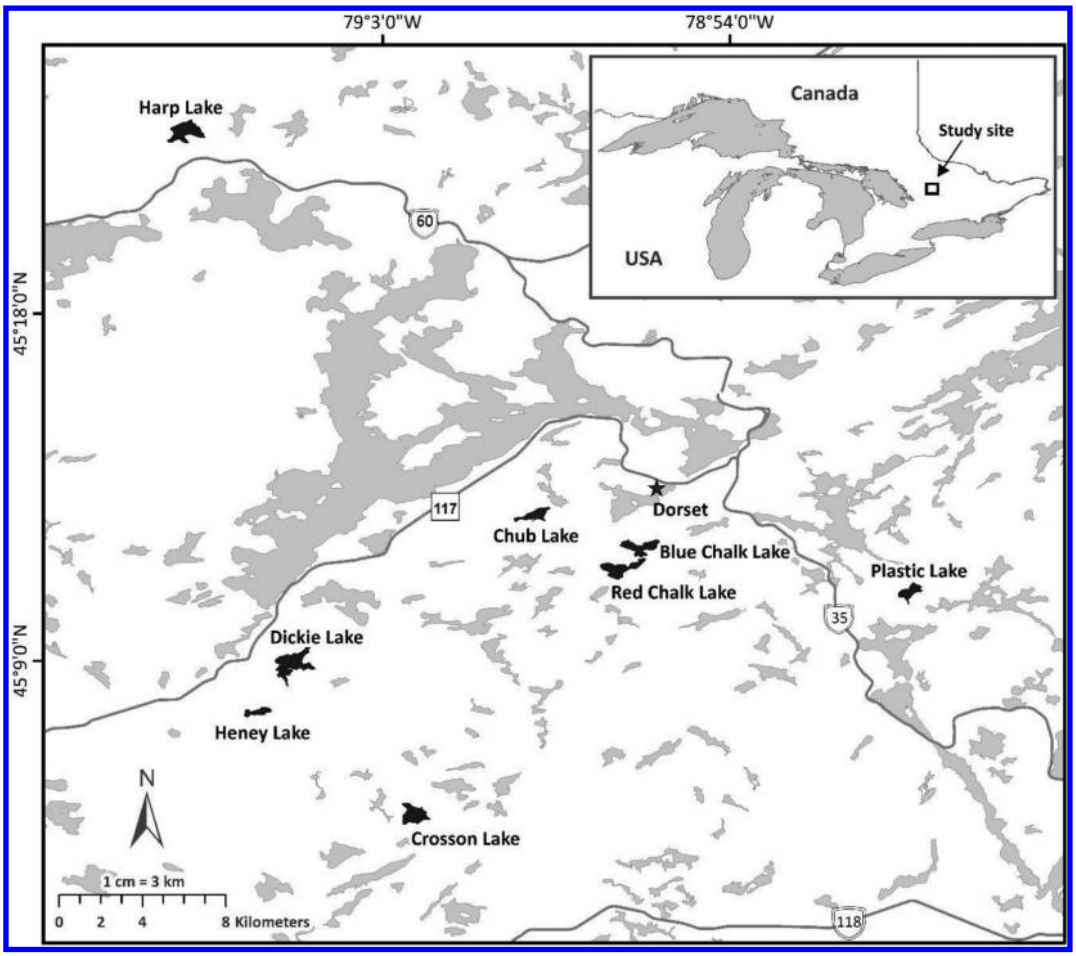

These eight lakes were chosen to be representative of Canadian Shield lakes in south-central Ontario.

Description of data

Field sampling and crustacean zooplankton identification counting and measurement techniques have been documented elsewhere (Rusak et al. 1999; Yan et al. 2008). Except for Dickie, Harp, and Plastic lakes, zooplankton samples were collected monthly during the ice-free season beginning in 1980. Harp and Plastic lakes were sampled every 2 weeks, while Dickie Lake was sampled monthly until 1988 and then every 2 weeks thereafter. Each sample was a bathymetrically weighted composite sample formed by taking four to seven vertical hauls with a 12.5 cm diameter, 80 μm mesh, conical, metered net from predetermined depths to the surface from a station located over the point of maximum depth in each lake. The lengths and number of hauls were chosen so that the lake strata contributed to the composite sample in approximate proportion to their volume.

A minimum of 250 individual crustacean zooplankton within each sample were identified to species or suborder (immature

copepods), measured for body length, and counted (Yan et al. 2008). The smallest crustacean zooplankton in our data set are copepod and calanoid nauplii and copepodites, bosminid cladocerans, *Alona* spp., *Chydorus* spp., *Alonella* spp., *Pleuroxus* spp., and *Scapholeberis kingi*. Larger zooplankton include cyclopoid and calanoid copepods and the cladocerans *Holopedium glacialis*, *Polyphemus pediculus*, *Daphnia* spp., *Sida crystallina*, and *Bythotrephes longimanus*. *Leptodora kindtii* was the largest zooplankton identified in the samples. Since daytime sampling was used, it is likely that *L. kindtii*'s biomass was underestimated. However, *L. kindtii* was found in 6% of the study lake samples, suggesting that their frequency of occurrence within these lakes is quite low. Once adjusted for underestimation of *L. kindtii* > 5 mm daytime biomass (Horppila et al. 2017), the percentage of total zooplankton biomass that is made up of *L. kindtii* > 5 mm, on average, is between 6% and 7%. Hence, we have slightly underestimated the biomass of *L. kindtii* > 5 mm but feel this would not introduce much bias into our results nor alter the patterns our analyses have revealed.

Construction of the zooplankton normalized abundance size spectrum (NASS)

For each zooplankton sample collected over the study period (1980–2011), we constructed the NASS. We decided to express zooplankter size as equivalent spherical diameter (ESD: diameter (μm) of a sphere that has the same cross-sectional area as the silhouette of a zooplankter), thus permitting direct comparison of our data with data generated by automated plankton counters (optical plankton counter (OPC) and Laser Optical Plankton Counter (LOPC); Herman 1988, Herman et al. 2004). To convert each zooplankton length measurement into mass, we first calculated the area (*A*) of an ellipse having the length measurement (*L*) and aspect ratio (*f*) of a particular zooplankton (one of us (WGS) developed a ratio of 7.6 for *Leptodora kindtii*, whereas ratios of 1.6 and 3 were used for all other cladocerans and copepods, respectively; Finlay et al. 2007).

$$A = \frac{\pi \times L^2}{f} \quad (1)$$

Then, we determined the diameter of a sphere having the same cross-sectional area (ESD).

$$\mathrm{ESD} = \frac{\sqrt{4 \times A}}{\pi} \times 1000 \quad (2)$$

Next, we used eq. (3) to find the volume of an ellipsoid with major axis = ESD and minor axis = ESD/*f*:

$$V = \frac{\pi \times \mathrm{ESD}^3}{6 \times f^2 \times 10^6} \quad (3)$$

where *V* is the biovolume (μL). Finally, we converted *V* into fresh mass (μg) assuming a specific gravity of 1. We set the minimum mass over which the NASS was calculated to 0.2458 μg ($2^{-2.024}$ μg) because this was the smallest mass that was found in 95% of the samples. We removed 68 samples from our data set that had minimum masses greater than 0.2458 μg, leaving us with 1852 samples. The NASS was calculated by grouping all zooplankton masses into a $\log_2$ series of mass intervals beginning at a minimum mass of $2^{-2.024}$ μg (lower bound of first mass bin) and ending at the maximum mass in each sample, counting the number of zooplankton within each mass interval, and dividing by the volume of water filtered and the linear width of the mass bin. Dividing by the linear width of the mass bin normalizes the abundance within each bin (hence "normalized" abundance size spectrum) by removing the dependency of abundance on the width of the mass bin (White et al. 2008).

To characterize the shape of the linear zooplankton NASS, we used ordinary least squares (OLS) regression to estimate the slope (no.·L^{-1}·μg^{-2}) and the normalized abundance (no.·L^{-1}·μg^{-1}) at the midpoint of the eighth mass bin ($2^{5.476}$ μg; i.e., the "height" of the spectrum). This bin is roughly at the centre of the log size range and is uncorrelated with the slope, thus providing an independent measure of the relative total abundance of the size-structured community (Daan et al. 2005). To remove any ambiguity, we will use the term "OLS slope" when we refer to the slope of the NASS estimated using OLS regression. Despite recommendations for using the maximum likelihood estimate (MLE) of the type I Pareto exponent over the OLS slope to describe the decline in abundance with body size (White et al. 2008; Sprules and Barth 2016; Edwards et al. 2017), we found that the MLE is much more affected by residual variation around the NASS than is the OLS slope, so we used the latter (see Appendix A).

Statistical analyses

One of our primary objectives was to compare, using a common currency, the magnitude of variation in spectrum parameters associated with variation in time (months and years) and space (among lakes). We accomplished this by treating month, year, and lake as random effects in a random effects model designed to partition the variance in the height and the OLS slope of the NASS into separate portions due to variation in month, year, and lake (i.e., seasonal dynamics, temporal processes, and limnological lake characteristics, respectively; Fig. 2A). We went on to quantify the average seasonal pattern in the height and OLS slope of the NASS and determined whether it varied among lakes and years (Fig. 2B).

In this second analysis, since the factor month likely has a consistent effect on the zooplankton size spectrum because of periodicity in seasonal processes, we treated integer month as a fixed quantitative effect in a mixed effects model, with year and lake as random effects. We expected this model structure would capture the linear rate of change in the height and the OLS slope over the months of May to October. Finally, we determined the months in which the zooplankton NASS parameters deviated the least from the seasonal average (Fig. 2C). For each lake and year, we calculated the seasonal mean $\log_2$ height and OLS slope and subtracted these values from the observed value of $\log_2$ height and OLS slope for a particular month, lake, and year combination. We treated month as a categorical fixed effect and estimated the average deviation for each month from the seasonal mean in a fixed effects model. All random and mixed effects models were fit with the lmer function in the lme4 R package, while the fixed effects model was fit with the gls function in the nlme R package (Bates et al. 2017; Pinheiro et al. 2017).

We created conceptual illustrations to aid in interpretation of each random, mixed, and fixed effects analysis (Fig. 2). Random effects models (Fig. 2A) are used to the estimate the variance (σ^2) in a response (e.g., spectrum height) associated with changes in a factor of interest (e.g., month). The grey arrows indicate the deviation from the grand mean (b_0; e.g., the grand mean spectrum height) associated with a single instance of the random effect of month, year, or lake. The grey dashed curves indicate a random distribution of the response, where all random effects are point estimates from a vector of normally distributed values with a mean of zero and variances estimated by the model (i.e., $b \sim N(0, \sigma^2)$). The width of the dashed curve indicates the relative influence on the grand mean of each effect (small, medium, and large).

Mixed models (Fig. 2B) estimate both fixed and random effects. The fixed effect represents the linear rate of change in the response (e.g. OLS slope) across the variable month and characterizes the seasonal pattern consistent among the eight lakes and over the 30 years. The random effect of lake, for example, esti-

Fig. 2. Objectives for each of the three types of analyses with conceptual illustrations. Random effects models (A) are used to the estimate the variance (σ^2; width of curve indicating effect size) in a response (e.g., spectrum height) associated with changes in a factor of interest (e.g., month). Mixed models estimate both fixed (solid black line) and random (dashed grey lines) effects (B). The fixed effect represents the global seasonal pattern, while the random effect estimates variability in the seasonal pattern due to a factor of interest (e.g., lake) either through effects on the elevation (i.e., intercept) of the line (*i*), the slope (β_1) of the line (*ii*), or both. Fixed effect models (C) can be used to estimate means. This is illustrated with the mean response (e.g., deviation from seasonal mean OLS slope) (solid circles) and standard error (bars) for each level of the factor (e.g., month).

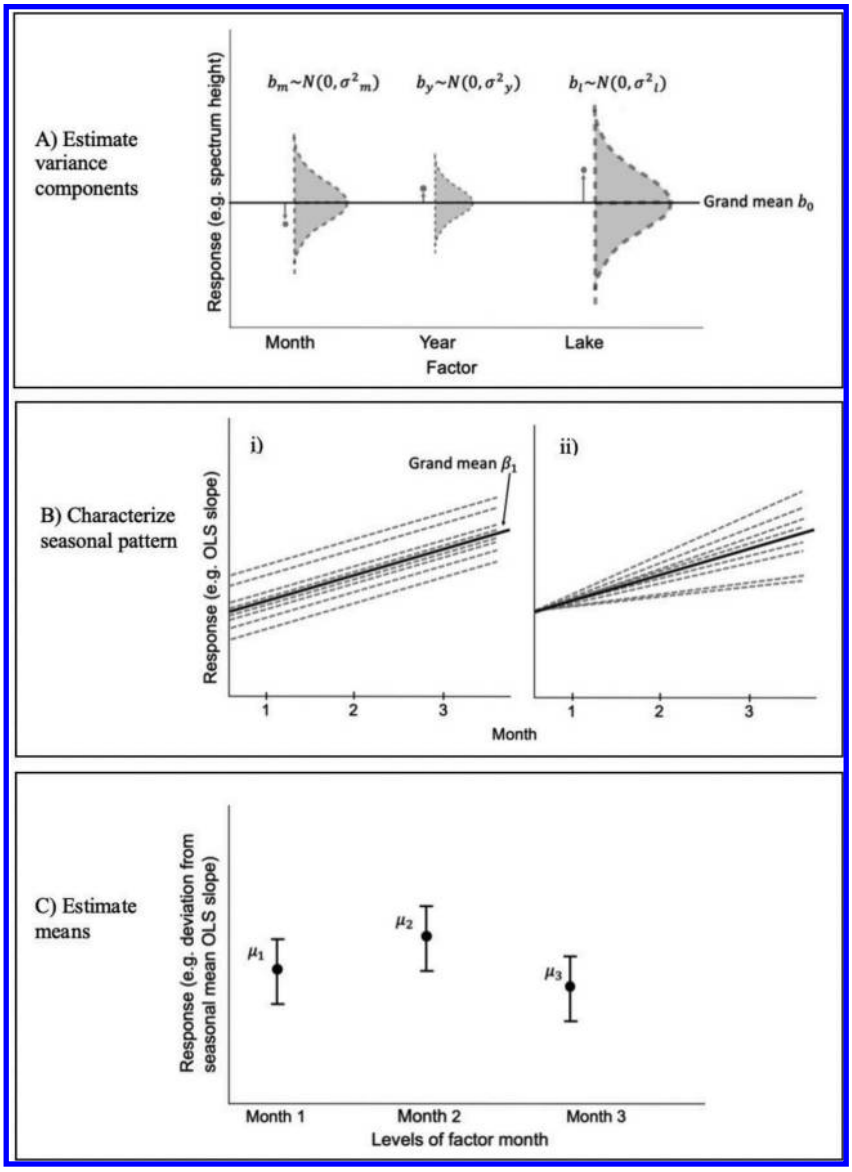

mates the variability around the grand mean seasonal pattern associated with the variable lake. This is illustrated by the eight dashed grey lines, with each line representing one of the eight lakes. The random effect of lake can affect the elevation (i.e., intercept) of the line (Fig. 2B*i*), the slope (β_1) of the line (Fig. 2B*ii*), or both. The random lake effect on the intercept and (or) slope is modelled by a normal distribution of values that reflect the relative variability in the intercept and slope observed among the lakes. Each of the grey dashed lines in Fig. 2B*i* or Fig. 2B*ii* represent the grand mean seasonal pattern adjusted by a single randomly selected value from the normal distribution modelling the variability in the intercept or slope due to the factor lake.

Fixed effect models (Fig. 2C) can be used to estimate means. When the factor (e.g., month) affecting a response (e.g., deviation from seasonal mean OLS slope) has specific values or characteristics (e.g., the month of May is typically colder), a fixed effect analysis based on maximum likelihood estimation is used to determine the mean and variability in the deviation from the seasonal mean OLS slope for each month.

Since we did not know the structure of the models needed for the first two parts of our analyses, we followed the procedures outlined in chapter 5 of Zuur et al. (2009) to determine the random components of these models. We created a set of 19 candidate random effects models, 14 candidate mixed effects models, and one fixed effects model. A detailed description of all candidate model components is provided in Appendix A (see Tables A1–A3). We selected the best-fit models using the minimum corrected Akaike information criterion (AIC_c), which balances the trade-off between model complexity and model fit. AIC_c values were computed using the AICc function in the MuMin R package (Bartoń 2015). Models with AIC_c differences ($\Delta_i(AIC_c)$) < 2, where $\Delta_i(AIC_c)$ is calculated as the minimum AIC_c value of the candidate models

Fig. 3. Mean ± standard error of the height (A) and OLS slope (B) of the zooplankton NASS for each of the Dorset lakes (Lake ID) averaged across years and months (n = 175 to 353 for each lake). Lake abbreviations: BC, Blue Chalk; CB, Chub; CN, Crosson; DE, Dickie; HP, Harp; HY, Heney; PC, Plastic; RCM, Red Chalk – main basin.

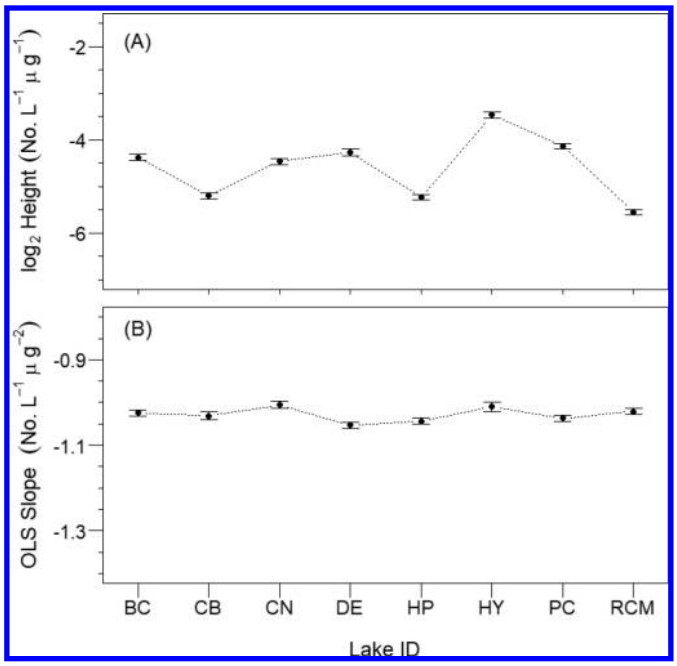

subtracted from each models AIC_c value, are models with substantial support as the "best" model compared with other candidate models (Burnham and Anderson 2004).

We used restricted maximum likelihood (REML) to estimate all effects in the first two analyses and maximum likelihood to estimate the fixed effects in the third analysis. In the mixed effect analysis, we centered integer month by subtracting seven from each month value (months May to October numbered 5 to 10, then subtract 7 = –2 to 3, respectively) to allow for a meaningful interpretation of the intercept of the model as the value of the response variable in July when most of the lakes are strongly stratified. Note, we use the REML estimate of the slope to characterize the linear rate of change in the NASS parameters over the season, which is different from the OLS slope, one of the NASS parameters. Our measures of model goodness of fit were the marginal and conditional coefficient of determination (R^2_M and R^2_C, respectively). R^2_M and R^2_C represent the proportion of variance explained by the fixed model components and the full model (i.e., random and fixed components), respectively (Nakagawa and Schielzeth 2013). R^2_M and R^2_C were computed using the sem.model.fits from the R package piecewiseSEM (Lefcheck 2016).

To compare variance components, we calculated both the total and relative variance explained per component. Total variance is the portion of the overall variance in the response variable attributable to a particular component of the model. For the random effects models, total variance is equivalent to the intraclass correlation coefficient. This coefficient for the month and year factors represent the synchronicity of these lakes over the season and across years (Rusak et al. 2002). Relative variance explained is a more intuitive metric than the total variance explained for determining which factors are important in accounting for variability in the response variable. It is calculated as follows: variance explained by a specific factor in the model / total variance explained by the model.

After the "best" model was identified, normality and homoscedasticity of the residuals were visually assessed using a normal probability plot and a residual versus fitted values plot, respectively. There were no patterns in the residuals that indicated heteroscedasticity, and the residuals approximated a normal distribution. However, one to five observations with unusually large residuals were removed and models were refit.

Table 2. Variance components and estimates of grand mean height and OLS slope of the zooplankton NASS from the best random intercept models.

Component	Grand mean	Var. (×100)	SD (×100)	% tot. var.	% rel. var.
Height of the NASS (no.·L⁻¹·µg⁻¹)					
Month	$2^{-4.616}$	13.58	36.84	9.9	13.6
Year		9.53	30.87	6.9	9.5
Lake		45.86	67.72	33.3	45.8
Month × year		7.05	26.55	5.1	7.0
Month × lake		4.73	21.74	3.4	4.7
Year × lake		14.65	38.27	10.6	14.6
Month × year × lake		4.70	21.69	3.4	4.7
Residual		37.66	61.37	27.3	
OLS slope of the NASS (no.·L⁻¹·µg⁻²)					
Month	–1.029	0.10	3.09	6.8	17.2
Year		0.06	2.53	4.5	11.5
Lake		0.01	0.96	0.7	1.7
Month × year		0.06	2.37	4.0	10.1
Month × lake		0.05	2.21	3.5	8.8
Year × lake		0.16	4.01	11.4	28.9
Month × year × lake		0.12	3.49	8.6	21.9
Residual		0.86	9.27	60.7	

Note: Total variance (Var.) was calculated as a sum of the variance explained by each component. Percent total variance explained (% tot. var.) is equivalent to the intraclass correlation coefficient (ICC; refer to Table A2). Percent relative variance explained (% rel. var.) was calculated relative to the amount of variance explained by the model (i.e., not including residual variance). SD, standard deviation.

Results

Random effects model: partitioning variability

Model selection using AIC_c revealed two "best" random intercept models that explained variability in the height of the NASS. These models included independent random effects of month, year, and lake, as well as their two-way interactions. The difference between the two models is the inclusion of a three-way interaction term (see Tables A1 and A4). We will limit the presentation of our results to the model including the three-way interaction. For the OLS slope of the NASS, the best random intercept model resembled that found for the height with the three-way interaction term. The random effects models explained 73% of total variability in the height and 39% of total variability in the OLS slope of the NASS (Table 2). The coefficient of variation (CV) for the height and the OLS slope provides relative measures of variance; the observations of height were more dispersed than that of the OLS slope (CV_{height} = 25%, CV_{Slope} = 12%).

For the height of the zooplankton NASS, the component that explained the largest amount of relative variance in these data was lake, suggesting that much of the variability in the height explained by the model was spatial in origin (Table 2; Fig. 3A). The year × lake random effect explained the second largest amount of relative variation in the height, but still much less than the lake effect, indicating that there was a lake-specific temporal effect that introduces asynchrony in the height among these lakes over time (Fig. 4). There does appear to be a small "global" temporal effect that influences the height in a similar way among lakes. The factor month explained the third largest amount of relative variation in the height, indicating that there was a global seasonal signal among these lakes, where the height from each lake tended to respond to seasonal dynamics in a consistent way (Fig. 5). The relatively small amount of variance explained by the month × year

Fig. 4. Long-term patterns in the yearly mean ± standard error estimate of the height of the zooplankton NASS, 1980–2011. Lake abbreviations as in Fig. 3.

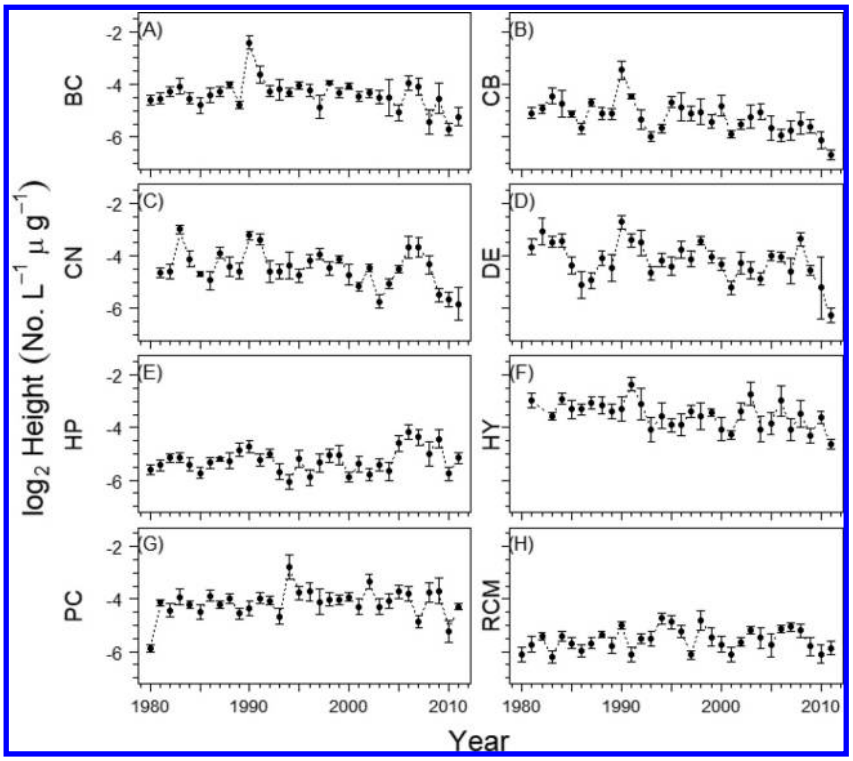

Fig. 5. Seasonal pattern in the height of the zooplankton NASS, showing mean ± standard error of the height across the months of May to October for each of the Dorset lakes (n = 24 to 63 for each lake and month combination). Lake abbreviations as in Fig. 3.

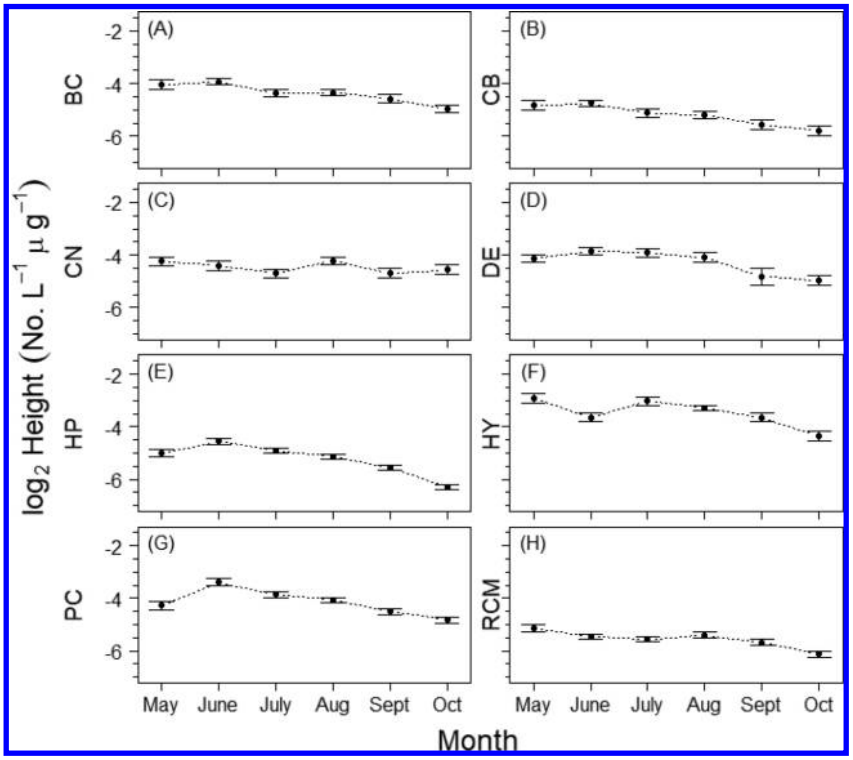

and month × lake interactions suggest that the seasonal pattern of height does not vary much among years or lakes. The variance explained by the month × year × lake interaction was relatively minor, indicating that the year-specific seasonal height pattern did not vary much among lakes.

By contrast, the lake component explained the least amount of variance in the OLS slope (Table 2; Fig. 3B). Thus, there appears to be little spatial variability in the OLS slope among these lakes. There seems to be a global seasonal signal in the OLS slope, as approximately 17% of the relative variability was explained by the

Fig. 6. Seasonal pattern in the OLS slope of the zooplankton NASS, showing mean ± standard error of the OLS slope across the months of May to October for each of the Dorset lakes. Lake abbreviations as in Fig. 3.

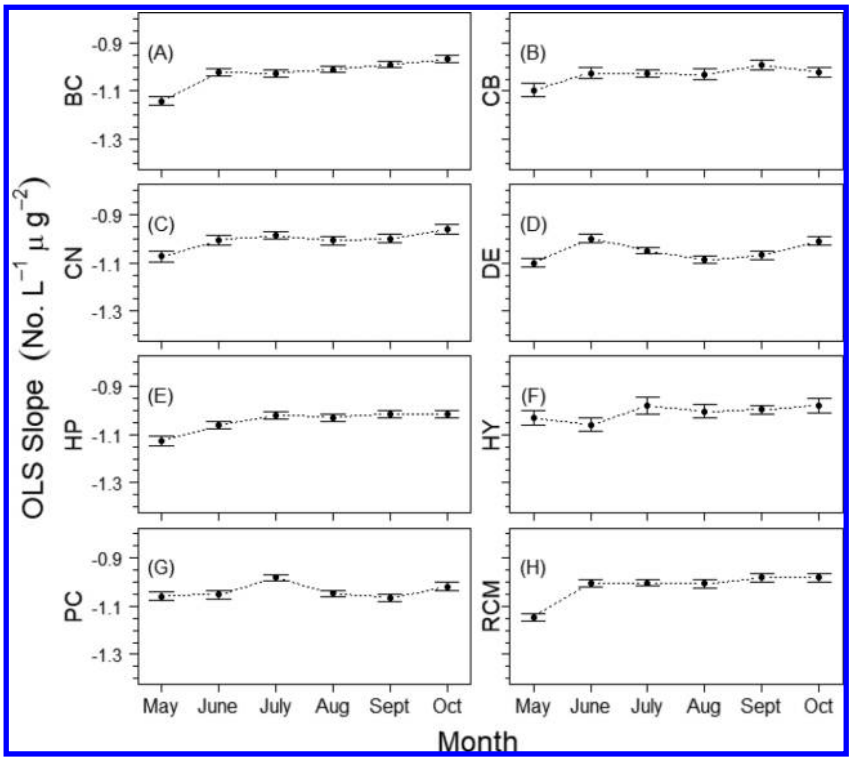

factor month (Figs. 6 and A2). However, the lake- and year-specific seasonal signal is greater than the global seasonal signal, as 40.8% of the relative variance is caused by the month × lake, month × year, and the month × year × lake interactions. This suggests that the seasonal signal of the OLS slope varies in a complex manner especially across lakes and years. There is little evidence of synchrony in the fluctuations of the OLS slope among lakes over years (i.e., small global year effect). The year × lake interaction explained the largest percentage of relative variance in the OLS slope, implying that temporal variation was lake-specific (Fig. 7). Owing to a large proportion of the relative variance attributed to these complex interactions in this model, it is difficult to make clear interpretations of OLS slope dynamics in terms of spatial, temporal, and seasonal processes. Furthermore, there is high residual variation and weak global patterns, suggesting that there is little synchrony in the OLS slope, at least within the effects measured.

Mixed effects model: describing seasonal pattern

To capture the global seasonal pattern in the height and the OLS slope, we looked at how these parameters changed over the months of May to October using mixed effects models. Plotting the mean ± SE (across lakes and years) of these parameters reveals a trend of decreasing height and increasing OLS slope over the ice-free season (Fig. A2). There is some evidence of curvature in the seasonal trend of both the height and the OLS slope. However, most of the seasonal pattern does appear to be linear. Hence, we explored whether this global linear change in height and OLS slope over the season was consistent across lakes and years by adding random effects to the linear seasonal trend in our mixed effects models (Fig. 2B).

The best mixed effects model for both the height and the OLS slope is commonly referred to as a random intercept (Fig. 2B.*i.*) and slope (Fig. 2B.*ii.*) model where each random factor can have an effect on both the intercept and the slope (Zuur 2009). The final model includes an intercept (i.e., grand mean response), the average linear change in the response (e.g., OLS slope) with the random effects of year and lake, and their two-way interaction, on this linear change and the intercept (Tables A1 and A5). Since we centered the values for integer month (C_{month}) on "July", the mean height or OLS slope in July is represented by the intercept estimate for the model.

Very little relative variability explained by the random factors was attributable to their effects on the linear rate of change in both the height and the OLS slope (sum of percent relative variance explained = ~4% and ~8%, respectively; Table 3). Most of the relative variability explained by these random factors was through their effects on the intercept (i.e., the mean height or mean OLS slope in July; ~96% and ~92%, respectively; Table 3).

When looking at the intercepts in the mixed effects models, we find similar results as the random effects models. The mean height in July appears to be most affected by factors related to among-lake differences (Table 3). There is some evidence of a small global temporal effect. However, the year × lake interaction suggests that there is a stronger lake-specific temporal effect influencing the mean height in July. The mean OLS slope in July does not appear to be influenced by among-lake differences. There is a global temporal effect, but the strongest effect comes from the year × lake interaction, suggesting that the relative variability explained by the model is largely driven by lake-specific, annual-scale factors on the intercept once seasonality is controlled.

It must be noted that the random effects models for both the height and the OLS slope of the NASS had lower AIC_c values than the corresponding mixed effects models (Tables A4 and A5). There was also a relatively large decline in the amount of total variability in the OLS slope explained by the mixed effects model relative to the random effects model (from ~39% down to ~23%), while there was only a small decline in explained total variability for the height (from ~70% down to ~63%).

Fig. 7. Long-term patterns in the yearly mean ± standard error estimate of the OLS slope of the zooplankton NASS, 1980–2011. The dotted black vertical line in panel (E) identifies the year when *Bythotrephes longimanus* invaded Harp Lake. Lake abbreviations as in Fig. 3.

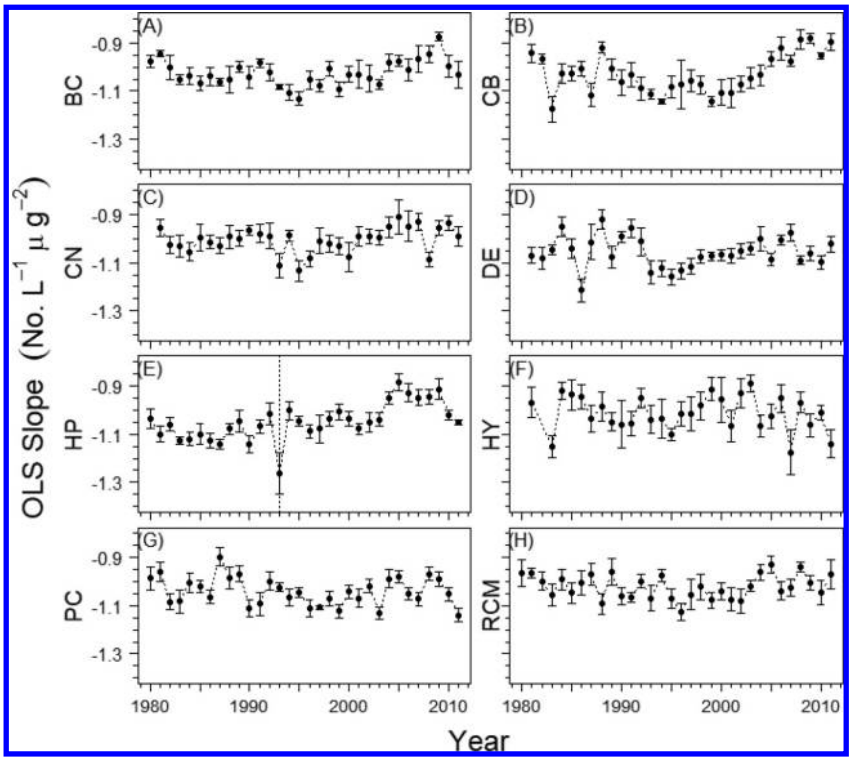

Table 3. Fixed effect estimates for the intercept and linear rate of change (Lin.Δ) of the "best" mixed effects model as well as variance estimates for the random factors in the mixed effects model for the height and the OLS slope of the zooplankton NASS.

Fixed effect name	Fixed effect estimate	Random factor name	Random effect on intercept or Lin.Δ	Variance (×1000)	SD (×100)	% total variance	% relative variance
Height of the NASS							
Intercept	−4.511						
Lin.Δ	−0.179						
		Year	Intercept	93.10	30.51	7.7	12.5
			Lin.Δ	14.45	12.02	1.2	1.9
		Lake	Intercept	463.74	68.10	38.3	62.4
			Lin.Δ	3.86	6.22	0.3	0.5
		Year × lake	Intercept	157.62	39.70	13.0	21.2
			Lin.Δ	10.25	10.12	0.8	1.4
		Residual		467.39	68.37	38.6	
OLS slope of the NASS							
Intercept	−1.036						
Lin. Δ	0.014						
		Year	Intercept	0.99	3.14	7.5	32.6
			Lin.Δ	0.03	0.52	0.2	0.9
		Lake	Intercept	0.14	1.19	1.1	4.7
			Lin.Δ	0.07	0.83	0.5	2.3
		Year × lake	Intercept	1.67	4.09	12.6	55.1
			Lin.Δ	0.13	1.15	1.0	4.4
		Residual		10.21	10.11	77.1	

Note: Details for calculation of total variance, percent total variance, and relative variance explained is described in Table 2.

Fixed effects model: minimizing seasonality

We wanted to determine in which months zooplankton sampling efforts should be focused to minimize the influence of seasonal dynamics of the zooplankton community on the estimates of the size spectrum parameters. For the height, we found that sampling early to midseason (except June) produced height estimates that were relatively similar to the seasonal mean (Fig. 8A; Table A7). However, later in the season (September to October), estimates of height were significantly lower than the seasonal mean. For the OLS slope, sampling from June to September produced estimates that were roughly similar to the seasonal mean OLS slope (Fig. 8B). However, sampling in May produced significantly steeper (i.e., more negative) estimates of OLS slope than the seasonal mean, while sampling in October produced significantly shallower (less negative) estimates of the OLS slope compared with the seasonal mean.

Fig. 8. Mean deviation from seasonal mean (value – seasonal mean) for the height (A) and the OLS slope (B) of the NASS across the season (n = 278 to 327 for each month). Error bars represent 95% confidence intervals. Error bars that cross the solid line identify months in which, on average, the seasonal mean is equal to the monthly height or OLS slope value.

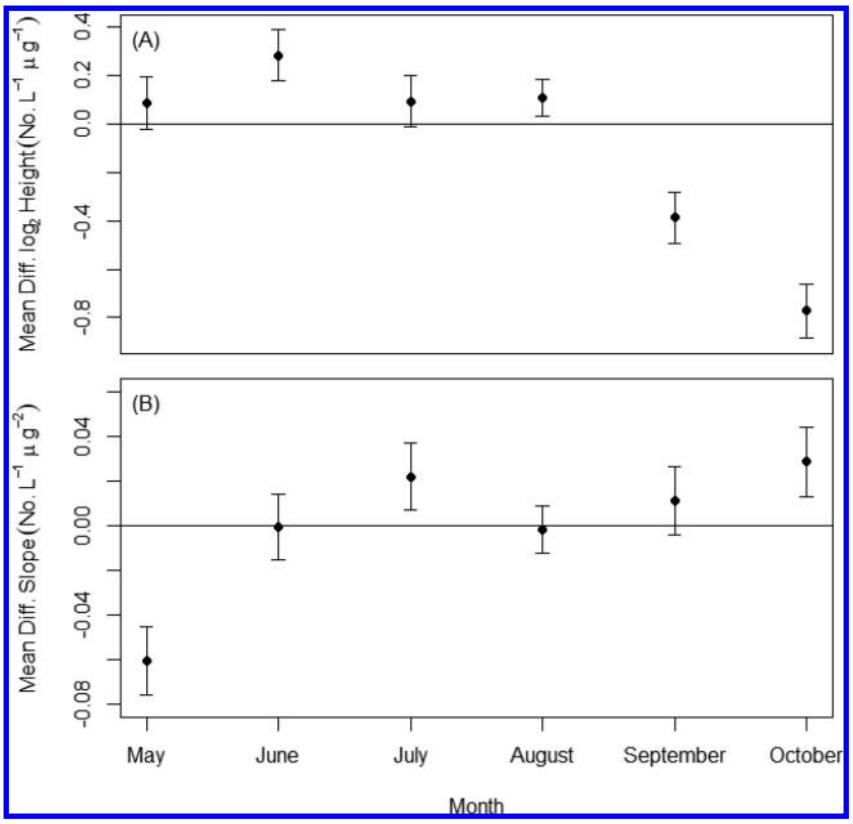

Discussion

Our analyses of the zooplankton size spectra in eight south-central Canadian Shield lakes showed that the OLS slope of the NASS varied much less than the height. Of the variance accounted for by our models, the height varied largely according to among-lake differences, while the OLS slope varied in a complex manner with most of the relative variance partitioned into the interactions. Residual error was quite high for the OLS slope models, suggesting that there was much unexplained variability. We identified a signal of systematic month-to-month change for both the height and the OLS slope with the random effects models. The linear decline in the height over the season appeared to be relatively consistent across lakes and years, as indicated by the mixed effects model, while the linear increase in the OLS slope was not.

Spatial, temporal, and seasonal variability

Height

Both random and mixed effects models accounted for relatively similar amounts of variability in the height, explaining about ⅔ of the total variance in the height. In regard to partitioning variability among spatial and temporal broad-scale factors, our results are consistent with our predictions. We found a predominance of spatial- over temporal-scale factors influencing the variance in height with 33% of the total variability occurring among lakes. Rusak et al. (2002) partitioned variance in pelagic crustacean zooplankton abundance for ten functional groups (e.g., large calanoids and small cladocerans) and four large taxonomic aggregates (e.g., cyclopoid copepods) among years, lakes, regions, and their interactions. Their data set comprised 22 lakes in three regions of central North America sampled over a period of 5 to 18 years. Similar to our results, they found that spatial variation dominated their analysis, with among-lake variation (within region) explaining the largest amount of variance (on average ~50% of total variance explained) and regional variation explained about half that found among lakes. This consistency with our results suggests that the height of the zooplankton spectrum is a good proxy for zooplankton abundance patterns.

It is generally thought that top-down (i.e., predation) pressures exert the strongest influence on the body size composition of zooplankton communities (O'Brien 1979), while the interaction between bottom-up (i.e., nutrient) and top-down forces influence the abundance of zooplankton communities (McQueen et al. 1989). Thus, exploration of lake-specific factors accounting for the observed variability in the height should look at both bottom-up factors related to lake morphometry and lake trophy and top-down factors such as fish predation pressure.

The second largest component explained by the random effects model, although much less than the lake component, was the interaction between year and lake (~11% total variability). This implies asynchrony in the interannual fluctuations of zooplankton community abundance among lakes within the same region. The zooplankton communities within these lakes have been exposed to both a changing climate and changes in water quality over time (e.g., ice cover (Yao et al. 2013), pH (Yan et al. 2008), dissolved organic carbon (Keller et al. 2008), TP (Eimers et al. 2009), and calcium (Molot and Dillon 2008)). We observed a small global interannual effect on the height (6.8% total variability) influencing all lakes in a similar manner, which may be in response to regional and global climate related variables. Synchrony in year-to-year fluctuations in the abundance of certain zooplankton species has been related to both global (El Nino – Southern Oscillation, Madden–Julian Oscillation) and regional (temperature, precipitation, ice cover) climate variables (Rusak et al. 2008). The stronger lake-specific annual effect on the height suggests that

either lakes within the same region may be responding differently to the same climate forcing or there is variability in the magnitude and direction of water quality changes among these lakes affecting the zooplankton communities differently, or some combination of the two.

We identified synchrony in the month-to-month fluctuations of the height among the Dorset lakes (~10% total variability). The decline in the height over the ice-free season appears to be a relatively conserved pattern among years and lakes (Fig. A2A). Given the only slightly better fit of the random versus mixed effects model for the height, we believe that the decline in height over the season is a real phenomenon reflecting patterns in nutrient flux and planktonic seasonal succession. Our observation of greatest heights in spring and then a decline over the season is consistent with seasonal successional patterns in zooplankton abundance (Sommer et al. 1986). In spring there is a high input of fresh water from snow melt carrying nutrients and organic compounds from the watershed into the lake (Mcknight et al. 1990). Nutrients contained within this snow melt runoff can be an order of magnitude greater than that in rain event loads. This allochthonous input combined with spring turnover results in high total phytoplankton and zooplankton abundances after ice-out (Judd et al. 2005). As these nutrients become depleted, and with less allochthonous input from rainwater, there is a shift toward larger inedible phytoplankton and total abundance of zooplankton declines (Sommer et al. 1986).

OLS slope

The random effects model explained much less total variance in the OLS slope (~39%) compared with the height. The mixed effects model, which fit a linear trend to the change in OLS slope over the ice-free season, did a poor job of explaining that variability (~23%). Thus, the residual error for both random and mixed effects models was quite high. The OLS slope of the zooplankton size spectrum did not vary by much, and the variation it did exhibit was not well captured by our spatial and temporal broad-scale factors. Since our factors were broad, incorporating all among-lake, -month, and -year variables, it may be that within-lake processes are generating the unexplained variance in the relative abundance of large- and small-bodied zooplankton. Within-lake spatial heterogeneity in zooplankton is generated by a variety of biological (e.g., predator avoidance) and physical (e.g., wind-induced water circulation) drivers over a wide range of spatial scales (Folt and Burns 1999). Since zooplankton samples were collected from a single station located at the deepest spot for each of the study lakes, within-lake spatial variability in different sizes of zooplankton could be responsible for most of the variance observed being partitioned into the residuals.

For the OLS slope, we did not find a predominance of spatial- over temporal-scale factors as we had predicted. In fact, very little variability in the OLS slope was spatial in origin (0.7% total variability). The study lakes are similar in terms of geologic history, bedrock, surface area, and climate, but they differ in mean depth and their abundance of planktivorous fish and invertebrates, which has been shown to strongly influence the size composition of zooplankton communities (O'Brien 1979; Dini and Carpenter 1992; Lagergren et al. 2008). Despite the strong evidence toward top-down pressures exerting strong control over zooplankton community body size, which differs considerably for the study lakes, we found no evidence that OLS slope reflects this trophic organization. Sprules (2008) compared the full pelagic community size spectra (phytoplankton, zooplankton, fish) of Lake Ontario with that of the tropical Lake Malawi in Africa, two completely different lakes with the only similarity being their size. He noted that the size spectra were remarkably similar and that slopes fitted to these size spectra were not significantly different. These observations of very different lake communities producing indistinguishable size spectra imply an inherent regulation of the abundance–body size relationship of biological communities beyond fine-scale ecological interactions.

We found a small amount of year-to-year variation in OLS slope that was consistent among lakes (4.5% total variability), but, as with the height, the interaction between year and lake effects was greater (11.4%). Thus, temporal variation in the OLS slope tends to be lake-specific. Interannual variability in the relative abundance of small- and large-bodied zooplankton could be related to changes in environmental characteristics of these lakes. Some investigators have found that the slope of the plankton size spectrum becomes flatter (less negative) with increasing lake productivity (i.e., phosphorus) (Sprules and Munawar 1986; Ahrens and Peters 1991). In productive systems, nutrients entering at a high rate are quickly cycled through nanoplankton with high turnover rates to produce a relatively high abundance of zooplankton grazers. This results in a greater amount of energy transferred up the food web to larger organisms. In less productive systems, nutrients entering at a lower rate are cycled through nanoplankton more slowly, producing a lower abundance of zooplankton grazers (Sprules and Munawar 1986). Thus, decline in TP in these already nutrient-poor Canadian Shield lakes could have profound consequences on energy flow up the food web, which may be reflected in the variability in the OLS slope we observed through time.

Most of the variance in the OLS slope that was explained by our model was associated with month-to-month variability. There was a small amount of seasonal variability that was consistent among lakes (6.8% total variance), but most of this variability was partitioned into the interactions (~16% total variance), suggesting that the seasonal signal was quite variable among lakes and through time. The random effects model is clearly better at explaining variability in OLS slope, suggesting that a fixed linear increase does not well capture the seasonal dynamics in the OLS slope.

The increase in the OLS slope observed over the season appears to be strongly influenced by a single month, May (Fig. A2). We performed a post hoc one-way analysis of variance (ANOVA) on the OLS slope using month as the predictor variable for each lake. Results of pairwise comparisons using Tukey's HSD test showed that three of the eight lakes (Blue Chalk, Harp, Red Chalk) showed significantly lower OLS slopes in May compared with all other months, while the rest of the months did not significantly differ from each other. Heney Lake did not significantly differ in OLS slope across any months. The last four lakes (Chub, Crosson, Dickie, Plastic) displayed fluctuating patterns across months, with three of these lakes showing a common trend of significantly lower OLS slopes in May compared with months later in the season. The patterns we observed in the OLS slope across the eight study lakes have been observed by other researchers. Random seasonal fluctuations in the plankton size spectrum slope was observed by Gasol et al. (1991), while steeper slopes in early spring compared with the rest of the season was noted by Gaedke (1992). Gaedke (1993) explained their observation of steep slopes in spring as an indication of inefficient energy transfer to higher trophic levels because of differences in generation times of the organisms involved in the food web. Zooplankton that respond quickly to the spring phytoplankton bloom are generally small, fast-growing herbivores that do not efficiently couple the energy pathway between trophic levels, resulting in a more negative slope. However, as larger herbivores with longer generation times become more abundant, the energy contained within the phytoplankton spring bloom is efficiently grazed upon and transferred up the food web to larger organisms, resulting in a less negative slope. Our results suggest that spring conditions can influence the zooplankton community size spectrum in a way that produces a steeper OLS slope, but the seasonal trend of the slope can be quite variable among lakes.

Inferences for sampling protocols

We have assessed seasonal variability in both the height and the OLS slope of the zooplankton NASS. Seasonal variance is greater than annual variance for both parameters, suggesting that long-term monitoring of lakes and interlake comparisons using zooplankton size spectra should standardize sampling protocols to minimize the effects of seasonal processes. If we assume the seasonal mean estimates of the height and the OLS slope reflect the zooplankton community near steady state, then sampling the zooplankton community in July–August tends to produce size spectrum estimates that tend to, on average, cancel out any effects of the seasonal succession processes occurring within zooplankton communities. Sampling earlier in the season could produce slope estimates significantly steeper than the seasonal mean, while sampling later in the season could produce height estimates significantly lower than the seasonal mean. These results can be generalized to other temperate lakes that exhibit seasonal changes in nutrient concentrations related to the spring thaw and turnover. All of the lakes we included in our analyses are relatively small, oligotrophic Canadian Shield lakes, but Gaedke (1992) also observed a similar seasonal pattern in the slope in Lake Constance, a large, deep, meso-eutrophic lake in Europe. Hence, a steep slope in spring appears to be a relatively common feature of temperate lakes. It is preferable to sample a lake multiple times throughout the ice-free season, but for large surveys, such as that by the Ontario government's Broad-scale Monitoring (BsM) program, the number of lakes that can be visited each year is limited by the frequency of sampling. If the objective of a sampling program is to compare or monitor a large number of lakes, then the ability of the size spectrum to reflect average-lake conditions is improved if sampling of zooplankton communities is focused on midsummer.

If the zooplankton size spectrum is to be used as a monitoring tool, we must first demonstrate that it actually responds to environmental perturbations. Theory predicts that perturbed spectra will return to a steady state if there are no further perturbations, with the time course of recovery being dependent on many size-based interactions and processes and their parameter values (Law et al. 2009; Rossberg 2012). One of the study lakes, Harp Lake, was invaded by the zooplanktivorous spiny water flea, *Bythotrephes longimanus*, in 1993, which caused major changes in the crustacean zooplankton community (Yan and Pawson 1997). With the Dorset data set, we have a known perturbation with multiple years of data before and after the invasion. This allows us to assess the ability of the OLS slope to respond to a strong perturbation as well as theoretical predictions about the ephemeral nature of perturbed spectra. The Harp Lake time series shows an abrupt change in the OLS slope of the zooplankton size spectrum in 1993, with a recovery to pre-invasion values by the next year (Fig. 7E). This observation highlights the stability of the slope of the size spectrum, but suggests that it will respond to a strong perturbation.

Conclusion

There is interest in using the size spectrum of lower trophic levels as a long-term monitoring tool and indicator of environmental perturbation (International Joint Commission 2014). The utility of the zooplankton size spectrum as an indicator depends on (*i*) its ability to reflect the structure and function of a system (Dale and Beyeler 2001) and (*ii*) our ability to distinguish between the typical range of variation related to spatial and temporal processes and the variation associated with extreme events (e.g., invasion of *Bythotrephes*) and long-term changes related to disturbance (e.g., reduction in lake ice cover; Magnuson 2007). Hence, we quantified the typical range of variation in the size spectrum parameters to determine by how much we can expect these parameters to vary in relation to broad-scale factors. Our results show that the OLS slope was relatively stable compared with the height and that the variability we could account for with the factors in our model was related to processes that occur on a month-to-month scale. In contrast, the variance in the height was largely driven by among-lake differences. Our observation of the OLS slope reflecting a strong perturbation (i.e., *Bythotrephes* invasion) and then bouncing back to pre-invasion values is consistent with theoretical predictions about spectrum dynamics. The stability of the size spectrum suggests that the ability to detect perturbations using zooplankton size spectra requires frequent monitoring of the zooplankton community. Thus, long-term monitoring of lakes using zooplankton size spectra will require inexpensive and quick sampling and processing methods that allow for increased frequency of lake visits and number of lakes monitored. The next step in developing the zooplankton size spectrum into a monitoring tool is to identify the finer-scale factors that are related to the variance in the height and the OLS slope we have observed. This will provide insight into the ability of the height and the slope to reflect the ecological state of a system, as well as the different types of perturbations that could be detected.

Acknowledgements

We are grateful to NSERC for their support to LEB and BJS through the Canadian Network for Aquatic Ecosystem Services and through a Discovery Grant to BJS. We acknowledge the support of the University of Toronto through a fellowship to LEB and the Ontario province's Dorset Environmental Science Centre for providing zooplankton data necessary for these analyses.

References

Ahrens, M.A., and Peters, R.H. 1991. Patterns and limitations in limnoplankton size spectra. Can. J. Fish. Aquat. Sci. **48**(10): 1967–1978. doi:10.1139/f91-234. doi:, 10.1139/f91-234.

Bartoń, K. 2015. MuMIn: Multi-model inference. R package version 1.15.6.

Bates, D., Maechler, M., Bolker, B., Walker, S., Christensen, R.H.B., Singmann, H., et al. 2017. lme4: linear mixed-effects models using "Eigen" and S4. R package version 1.1-17.

Blanchard, J.L., Dulvy, N.K., Jennings, S., Ellis, J.R., Pinnegar, J.K., Tidd, A., and Kell, L.T. 2005. Do climate and fishing influence size-based indicators of Celtic Sea fish community structure? ICES J. Mar. Sci. **62**(3): 405–411. doi:10.1016/j.icesjms.2005.01.006.

Blanco, J.M., Echevarría, F., and García, C.M. 1994. Dealing with size-spectra: some conceptual and mathematical problems. Sci. Mar. **58**(1–2): 17–29.

Boudreau, P.R., and Dickie, L.M. 1992. Biomass spectra of aquatic ecosystems in relation to fisheries yield. Can. J. Fish. Aquat. Sci. **49**(8): 1528–1538. doi:10.1139/f92-169.

Burnham, K.P., and Anderson, D.R. 2004. Multimodel inference: Understanding AIC and BIC in model selection. Sociol. Methods Res. **33**(2): 261–304. doi:10.1177/0049124104268644.

Cohen, J.E., Pimm, S.L., Yodzis, P., and Saldana, J. 1993. Body sizes of animal predators and animal prey in food webs. J. Anim. Ecol. **62**(1): 67–78. doi:10.2307/5483.

Daan, N., Gislason, H., Pope, J.G., and Rice, J.C. 2005. Changes in the North Sea fish community: evidence of indirect effects of fishing? ICES J. Mar. Sci. **62**(2): 177–188. doi:10.1016/j.icesjms.2004.08.020.

Dale, V.H., and Beyeler, S.C. 2001. Challenges in the development and use of ecological indicators. Ecol. Indic. **1**(1): 3–10. doi:10.1016/S1470-160X(01)00003-6.

Dini, M.L., and Carpenter, S.R. 1992. Fish predators, food availability and diel vertical migration in *Daphnia*. J. Plankton Res. **14**(3): 359–377. doi:10.1093/plankt/14.3.359.

Edwards, A.M., Robinson, J.P.W., Plank, M.J., Baum, J.K., and Blanchard, J.L. 2017. Testing and recommending methods for fitting size spectra to data. Methods Ecol. Evol. **8**(1): 57–67. doi:10.1111/2041-210X.12641.

Eimers, M.C., Watmough, S.A., Paterson, A.M., Dillon, P.J., and Yao, H. 2009. Long-term declines in phosphorus export from forested catchments in south-central Ontario. Can. J. Fish. Aquat. Sci. **66**(10): 1682–1692. doi:10.1139/F09-101.

Emmrich, M., Brucet, S., Ritterbusch, D., and Mehner, T. 2011. Size spectra of lake fish assemblages: Responses along gradients of general environmental factors and intensity of lake-use. Freshw. Biol. **56**(11): 2316–2333. doi:10.1111/j.1365-2427.2011.02658.x.

Finlay, K., Beisner, B.E., and Barnett, A.J.D. 2007. The use of the Laser Optical Plankton Counter to measure zooplankton size, abundance, and biomass in small freshwater lakes. Limnol. Oceanogr. **5**(1): 41–49. doi:10.4319/lom.2007.5.41.

Folt, C.L., and Burns, C. 1999. Biological drivers of zooplankton patchiness. Trends Ecol. Evol. **14**(8): 300–305. doi:10.1016/S0169-5347(99)01616-X.

Gaedke, U. 1992. The size distribution of plankton biomass in a large lake and its

seasonal variability. Limnol. Oceanogr. **37**(6): 1202–1220. doi:10.4319/lo.1992.37.6.1202.

Gaedke, U. 1993. Ecosystem analysis based on biomass size distributions: A case study of a plankton community in a large lake. Limnol. Oceanogr. **38**(1): 112–127. doi:10.4319/lo.1993.38.1.0112.

Gamble, A.E., Lloyd, R., Aiken, J., Johannsson, O.E., and Mills, E.L. 2006. Using zooplankton biomass size spectra to assess ecological change in a well-studied freshwater lake ecosystem: Oneida Lake, New York. Can. J. Fish. Aquat. Sci. **63**(12): 2687–2699. doi:10.1139/f06-153.

Gasol, J.M., Guerrero, R., and Pedrós-Alió, C. 1991. Seasonal variations in size structure and procaryotic dominance in sulfurous Lake Cisó. Limnol. Oceanogr. **36**(5): 860–872. doi:10.4319/lo.1991.36.5.0860.

Gorokhova, E., Lehtiniemi, M., Postel, L., Rubene, G., Amid, C., Lesutiene, J., et al. 2016. Indicator properties of Baltic zooplankton for classification of environmental status within Marine Strategy Framework Directive. PLoS ONE, **11**(7): 1–26. doi:10.1371/journal.pone.0158326.

Great Lakes Water Quality and Science Advisory Boards. 2013. Great Lakes ecosystem indicators — summary report: the few that tell us the most [online]. Available from http://www.ijc.org/files/publications/SummaryReport_EcoIndicators_2013.pdf.

Hansson, L.A., Gustafsson, S., Rengefors, K., and Bomark, L. 2007. Cyanobacterial chemical warfare affects zooplankton community composition. Freshw. Biol. **52**(7): 1290–1301. doi:10.1111/j.1365-2427.2007.01765.x.

Herman, A.W. 1988. Simultaneous measurement of zooplankton and light attenuance with a new optical plankton counter. Cont. Shelf Res. **8**(2): 205–221. doi:10.1016/0278-4343(88)90054-4.

Herman, A.W., Beanlands, B., and Phillips, E.F. 2004. The next generation of Optical Plankton Counter: the Laser-OPC. J. Plankton Res. **26**(10): 1135–1145. doi:10.1093/plankt/fbh095.

Horppila, J., Laakso, S., Niemistö, J., and Nurminen, L. 2017. Size-specific net avoidance behavior leads to considerable under-estimation of the biomass of *Leptodora kindtii* during day time sampling. Int. Rev. Hydrobiol. **102**(5–6): 151–158. doi:10.1002/iroh.201701902.

International Joint Commission. 2014. Great Lakes ecosystem indicator project report [online]. Available from http://www.ijc.org/files/publications/Ecosystem Indicators-Final.pdf.

Jennings, S., Pinnegar, J.K., Polunin, N.V.C., and Boon, T.W. 2001. Weak cross-species relationships between body size and trophic level belie powerful size-based trophic structuring in fish communities. J. Anim. Ecol. **70**(6): 934–944. doi:10.1046/j.0021-8790.2001.00552.x.

Jeppesen, E., Jensen, J.P., Søndergaard, M., and Lauridsen, T. 2000. Trophic structure, species richness and biodiversity in Danish lakes: changes along a phosphorus gradient. Freshw. Biol. **45**(2): 201–218. doi:10.1046/j.1365-2427.2000.00675.x.

Jeziorski, A., Yan, N.D., Paterson, A.M., DeSellas, A.M., Turner, M.A., Jeffries, D.S., et al. 2008. The widespread threat of calcium decline in fresh waters. Science, **322**(5906): 1374–1377. doi:10.1126/science.1164949.

Judd, K.E., Adams, H.E., Bosch, N.S., Kostrzewski, J.M., Scott, C.E., Schultz, B.M., et al. 2005. A case history: Effects of mixing regime on nutrient dynamics and community structure in Third Sister Lake, Michigan during late winter and early spring 2003. Lake Reserv. Manag. **21**(3): 316–329. doi:10.1080/07438140509354437.

Keller, W. (Bill), Paterson, A.M., Somers, K.M., Dillon, P.J., Heneberry, J., and Ford, A. 2008. Relationships between dissolved organic carbon concentrations, weather, and acidification in small Boreal Shield lakes. Can. J. Fish. Aquat. Sci. **65**(5): 786–795. doi:10.1139/f07-193.

Kratz, T.K., Frost, T.M., and Magnuson, J.J. 1987. Inferences from spatial and temporal variability in ecosystems: long-term zooplankton data from lakes. Am. Nat. **129**(6): 830–846. doi:10.1086/284678.

Lagergren, R., Leberfinger, K., and Stenson, J.A.E. 2008. Seasonal and ontogenetic variation in diel vertical migration of *Chaoborus flavicans* and its effect on depth-selection behavior of other zooplankton. Limnol. Oceanogr. **53**(3): 1083–1092. doi:10.4319/lo.2008.53.3.1083.

Law, R., Plank, M.J., James, A., and Blanchard, J.L. 2009. Size-spectra dynamics from stochastic predation and growth of individuals. Ecology, **90**(3): 802–811. doi:10.1890/07-1900.1.

Lefcheck, J. 2016. piecewiseSEM: Piecewise structural equation modeling. R package version 1.2.1.

Magnuson, J.J. 2007. Perspectives on the long-term dynamics of lakes in the landscape. Lake Reserv. Manag. **23**(4): 452–456. doi:10.1080/07438140709354030.

McCann, K.S., Gellner, G., McMeans, B.C., Deenik, T., Holtgrieve, G., Rooney, N., et al. 2016. Food webs and the sustainability of indiscriminate fisheries. Can. J. Fish. Aquat. Sci. **73**(4): 656–665. doi:10.1139/cjfas-2015-0044.

McGarvey, R., Dowling, N., and Cohen, J.E. 2016. Longer food chains in pelagic ecosystems: trophic energetics of animal body size and metabolic efficiency. Am. Nat. **188**(1): 76–86. doi:10.1086/686880.

Mcknight, D.M., Smith, R.L., Bradbury, J.P., Baron, J.S., and Spaulding, S. 1990. Phytoplankton dynamics in three Rocky Mountain lakes, Colorado, U.S.A. Arct. Alp. Res. **22**(3): 264–274. doi:10.2307/1551589.

McQueen, D.J., Johannes, M.R.S., Post, J.R., Stewart, T.J., and Lean, D.R.S. 1989. Bottom-up and top-down impacts on freshwater pelagic community structure. Ecol. Monogr. **59**(3): 289–309. doi:10.2307/1942603.

Messager, M.L., Lehner, B., Grill, G., Nedeva, I., and Schmitt, O. 2016. Estimating the volume and age of water stored in global lakes using a geo-statistical approach. Nat. Commun. 13603. doi:10.1038/ncomms13603.

Mills, E.L., and Schiavone, A.J. 1982. Evaluation of fish communities through assessment of zooplankton populations and measures of lake productivity. North Am. J. Fish. Manag. **2**(1): 14–27. doi:10.1577/1548-8659(1982)2<14:EOFCTA>2.0.CO;2.

Modica, L., Velasco, F., Preciado, I., Soto, M., and Greenstreet, S.P.R. 2014. Development of the large fish indicator and associated target for a Northeast Atlantic fish community. ICES, **71**(9): 2403–2415. doi:10.1093/icesjms/fsu101.

Molot, L.A., and Dillon, P.J. 2008. Long-term trends in catchment export and lake concentrations of base cations in the Dorset study area, central Ontario. Can. J. Fish. Aquat. Sci. **65**(5): 809–820. doi:10.1139/f08-035.

Moore, S.K., and Suthers, I.M. 2006. Evaluation and correction of subresolved particles by the optical plankton counter in three Australian estuaries with pristine to highly modified catchments. J. Geophys. Res. Ocean. **111**(5): 1–14. doi:10.1029/2005JC002920.

Nakagawa, S., and Schielzeth, H. 2013. A general and simple method for obtaining R^2 from generalized linear mixed-effects models. Methods Ecol. Evol. **4**(2): 133–142. doi:10.1111/j.2041-210x.2012.00261.x.

O'Brien, W.J. 1979. The predator–prey interaction of planktivorous fish and zooplankton. Am. Sci. **67**(5): 572–581. Available from http://www.jstor.org/stable/27849438.

Patalas, K. 1990. Diversity of the zooplankton communities in Canadian lakes as a function of climate. SIL Proceedings, 1922–2010, **24**(1): 360–368. doi:10.1080/03680770.1989.11898759.

Pawson, T.W., and McEachern, L.J. 1987. *Chaoborus* abundance in Muskoka–Haliburton Lakes: 1986 methods and data. Ontario Ministry of the Environment Data Report, DR 87/3.

Peters, R.H. 1983. The ecological implications of body size. Cambridge University Press, New York.

Pinheiro, J., Bates, D., DebRoy, S., Sarkar, D., Heisterkamp, S., and Van Willigen, B. 2017. nlme: linear and nonlinear mixed effects models. R Package version 3.1-137.

Richardson, A.J. 2018. In hot water: zooplankton and climate change. ICES J. Mar. Sci. **65**(3): 279–295. doi:10.1093/icesjms/fsn028.

Rossberg, A.G. 2012. A complete analytic theory for structure and dynamics of populations and communities spanning wide ranges in body size. Adv. Ecol. Res. **46**: 427–521. doi:10.1016/B978-0-12-396992-7.00008-3.

Rusak, J.A., Yan, N.D., Somers, K.M., and McQueen, D.J. 1999. The temporal coherence of zooplankton population abundances in neighboring north-temperate lakes. Am. Nat. **153**(1): 46–58. doi:10.1086/303147.

Rusak, J.A., Yan, N.D., Somers, K.M., Cottingham, K.L., Micheli, F., Carpenter, S.R., et al. 2002. Temporal, spatial, and taxonomic patterns of crustacean zooplankton variability in unmanipulated north-temperate lakes. Limnol. Oceanogr. **47**(3): 613–625. doi:10.4319/lo.2002.47.3.0613.

Rusak, J.A., Yan, N.D., and Somers, K.M. 2008. Regional climatic drivers of synchronous zooplankton dynamics in north-temperate lakes. Can. J. Fish. Aquat. Sci. **65**(5): 878–889. doi:10.1139/f08-043.

Sheldon, R., and Parsons, T. 1967. A continuous size spectrum for particulate matter in the sea. J. Fish. Board Canada, **24**(5): 909–915. doi:10.1139/f67-081.

Sommer, U., Gliwicz, Z.M., Lampert, W., and Duncan, A. 1986. The PEG-model of seasonal succession of planktonic events in fresh waters. Arch. fur Hydrobiol. **106**(4): 433–471.

Sprules, W.G. 2008. Ecological change in Great Lakes communities — a matter of perspective. Can. J. Fish. Aquat. Sci. **65**(1): 1–9. doi:10.1139/f07-136.

Sprules, W.G., and Barth, L.E. 2016. Surfing the biomass size spectrum: some remarks on history, theory, and application. Can. J. Fish. Aquat. Sci. **73**(4): 477–495. doi:10.1139/cjfas-2015-0115.

Sprules, W.G., and Munawar, M. 1986. Plankton size spectra in relation to ecosystem productivity, size, and perturbation. Can. J. Fish. Aquat. Sci. **43**(9): 1789–1794. doi:10.1139/f86-222.

White, E.P., Enquist, B.J., and Green, J.L. 2008. On estimating the exponent of power-law frequency distributions. Ecology, **89**(4): 905–912. doi:10.1890/07-1288.1.

Xu, F.L., Tao, S., Dawson, R.W., Li, P.G., and Cao, J. 2001. Lake ecosystem health assessment: indicators and methods. Water Res. **35**(13): 3157–3167. doi:10.1016/S0043-1354(01)00040-9.

Yan, N.D., and Pawson, T.W. 1997. Changes in the crustacean zooplankton community of Harp Lake, Canada, following invasion by *Bythotrephes cederstroemi*. Freshw. Biol. **37**: 409–425. doi:10.1046/j.1365-2427.1997.00172.x.

Yan, N.D., Blukacz, A., Sprules, W.G., Kindy, P.K., Hackett, D., Girard, R.E., and Clark, B.J. 2001. Changes in zooplankton and the phenology of the spiny water flea, *Bythotrephes*, following its invasion of Harp Lake, Ontario, Canada. Can. J. Fish. Aquat. Sci. **58**(12): 2341–2350. doi:10.1139/f01-171.

Yan, N.D., Somers, K.M., Girard, R.E., Paterson, A.M., Keller, W. (Bill)., et al. 2008. Long-term trends in zooplankton of Dorset, Ontario, lakes: the probable interactive effects of changes in pH, total phosphorus, dissolved organic carbon, and predators. Can. J. Fish. Aquat. Sci. **65**(5): 862–877. doi:10.1139/f07-197.

Yao, H., Rusak, J.A., Paterson, A., Somers, K.M., Mackay, M., Girard, R., Ingram, R., and McConnell, C. 2013. The interplay of local and regional factors in generating temporal changes in the ice phenology of Dickie Lake, south-central Ontario, Canada. Inl. Waters, **3**(1): 1–14. doi:10.5268/IW-3.1.517.

Zuur, A.F., Elena, N.I., Walker, N.J., Saveliev, A.A., and Smith, G.M. 2009. Mixed effects moddelling for nested data. *In* Mixed effects models and extensions in ecology with R. Springer Science+Business Media, LLC, New York, USA.

Appendix A

Comparison of the OLS slope of the NASS with the MLE Pareto exponent

There has been criticism over binning methods used to estimate the slope of the size spectrum. It has been recommended that the exponent of the type I Pareto distribution be estimated using maximum likelihood estimation (MLE), over the ordinary least squares (OLS) slope of the normalized abundance size spectrum (NASS), to describe the decline in abundance with body size, but this recommendation is based on simulations of idealized linear spectra (White et al. 2008; Edwards et al. 2017). Thus, we explored which estimate is a better predictor of the decline in abundance with body size for spectra derived from real data.

Using an independent data set of 299 Canadian Shield lakes collected by the Broad-scale Lakes Monitoring (BsM) Program of the Ontario Ministry of Natural Resources and Forestry (OMNRF) (Sandstrom et al. 2013), we constructed the NASS from zooplankton community samples that were processed with an optical plankton counter. The NASS was constructed over eight mass bins corresponding to a mass range of $2^{2.654}$–$2^{10.654}$ μg (lower bound of first bin – upper bound of last bin), which equates to an equivalent spherical diameter (ESD) of 338.97–2152.50 μm. The OLS slope of the NASS was computed for each size spectrum. Over the same mass range, we computed the MLE of the type I truncated Pareto exponent using White et al.'s (2008) formula.

For each of the 299 lakes, we fit both a first- and second-order polynomial to the NASS using OLS regression and estimated the fit of the linear and quadratic model using the coefficient of determination (R^2). Size spectra often show secondary domes or quadratic patterns in nature (Sprules and Barth 2016). We took the difference between the quadratic and the linear R^2 and arranged these differences in descending order. The top 75 lakes (greatest difference) were designated as NASS with a quadratic structure and the bottom 75 lakes as a linear structure.

We computed two paired t tests to determine whether the OLS slope of the NASS and the MLE of the Pareto exponent were significantly different from each other when the NASS had (*i*) a quadratic structure and (*ii*) a linear structure. We found that the Pareto exponent and the OLS slope of the NASS were significantly different from each other for both the linear structure (mean difference = −0.09, t = −2.84, df = 74, p value = 0.005) and the quadratic structure (mean difference = −0.47, t = −8.18, df = 74, p value < 0.0001). However, the effect size observed was small for the linear NASS analysis (Cohen's d = 0.33; Sawilowsky 2017) and large for the quadratic NASS analysis (Cohen's d = 0.94), suggesting that the OLS slope and the Pareto exponent are more similar when the NASS has a linear structure.

Next, for each of the lakes we plotted the NASS fitted with the OLS regression line (Figs. A1A–A1B) as well as their corresponding rank-frequency plots fitted with a power law using the maximum likelihood estimate of the truncated Pareto exponent (Figs. A1C–A1D). A common feature of the nonlinear NASS lakes was an overestimation of the abundance of large-bodied zooplankton using the Pareto exponent (Figs. A1C–A1D), whereas estimates using the OLS slope of the NASS match observed data quite well (Figs. A1A–A1B). Thus, it appears that the OLS slope is a good descriptor of the decline in abundance with body size for all spectra, whereas the MLE is appropriate only for near linear spectra.

Random, mixed, and fixed effects models

To address our main objectives, we used (*i*) a random effects model to quantify the relative variance in the NASS OLS slope and the NASS height attributable to differences in month, year, and lake; (*ii*) a mixed effects model to determine the magnitude and consistency, across years and lakes, of seasonal patterns in the NASS height and NASS OLS slope; and (*iii*) a fixed effects model to identify those months where the NASS parameters deviated the least from their seasonal average. Since we did not know the random components to include in the random and mixed effects models, we used the procedure outlined in Zuur et al. (2009) to identify the most parsimonious model that explained variance in the height and the OLS slope of the NASS.

For the first two parts of our analyses, we created a set of 19 candidate random effects models, 14 candidate mixed effects models, and one fixed effect model (Table A1). We have provided a detailed description of all model components for the random (Table A2) and mixed (Table A3) effects models. We used the minimum corrected Akaike information criterion (AIC_c) to select the best random and mixed effects model. Models R18 and R19 (Table A1) were found to be the best random effects models for explaining variability in the height of the NASS, while model R19 was the single best random effects model for the OLS slope (Table A4). Model M12 (Table A1) was found to be the best mixed effects model for both the height and the OLS slope of the NASS (Table A5).

There was a significant global seasonal trend in both the height and the OLS slope of NASS over the months of May to October (Table A6; Fig. A2). There was a decline in the height and an increase in the OLS slope over the season. For the OLS slope of the NASS, a common feature of the lake-specific seasonal pattern is steeper (more negative) OLS slopes early in the season. The lake-specific seasonal pattern in the height of the NASS resembles that of the observed global seasonal pattern. Most lakes display a general decline in NASS height over the season.

For our third analysis we calculated the seasonal mean NASS $\log_2$ height and NASS OLS slope and subtracted these values from the observed value of NASS $\log_2$ height and NASS OLS slope for a particular month, lake, and year combination. We treated month as a categorical fixed effect and estimated the average deviation for each month from the seasonal mean in a fixed effects model. The coefficient for each month is an estimate of the deviation of that month from the overall seasonal mean value for the dependent variable.

We found that the height of the NASS was relatively similar to the seasonal mean height earlier in the season (May and July; Table A7), whereas estimates of height later in the season (September to October) were significantly lower than the seasonal mean. The OLS slope was similar to the seasonal mean from June to September, but sampling in May produced significantly steeper (i.e., more negative) estimates of OLS slope than the seasonal mean, while sampling in October produced significantly shallower (less negative) estimates of the OLS slope compared with the seasonal mean (Table A7).

References

Edwards, A.M., Robinson, J.P.W., Plank, M.J., Baum, J.K., and Blanchard, J.L. 2017. Testing and recommending methods for fitting size spectra to data. Methods Ecol. Evol. **8**(1): 57–67. doi:10.1111/2041-210X.12641.

Hansen, G.J.A., Hennessy, J.M., Cichosz, T.A., and Hewett, S.W. 2015. Improved models for predicting walleye abundance and setting safe harvest quotas in northern Wisconsin lakes. North Am. J. Fish. Manag. **35**(6): 1263–1277. doi:10.1080/02755947.2015.1099580.

Sandstrom, S., Rawson, M., and Lester, N. 2013. Manual of instructions for broad-scale fish community monitoring using North American (NA1) and Ontario small mesh (ON2) gillnets. Peterborough, Ontario. Version 2013.2 35.

Sawilowsky, S.S. 2017. New effect size rules of thumb. J. Mod. Appl. Stat. Methods, **8**(2): 597–599. doi:10.22237/jmasm/1257035100.

Sprules, W.G., and Barth, L.E. 2016. Surfing the biomass size spectrum: some remarks on history, theory, and application. Can. J. Fish. Aquat. Sci. **73**(4): 477–495. doi:10.1139/cjfas-2015-0115.

White, E.P., Enquist, B.J., and Green, J.L. 2008. On estimating the exponent of power-law frequency distributions. Ecology, **89**(4): 905–912. doi:10.1890/07-1288.1. PMID:18481513.

Zuur, A.F., Elena, N.I., Walker, N.J., Saveliev, A.A., and Smith, G.M. 2009. Mixed effects moddelling for nested data. *In* Mixed effects models and extensions in ecology with R. Springer Science+Business Media, LLC, New York, USA.

Fig. A1. Zooplankton normalized abundance size spectrum (A–B) fitted with the ordinary least squares (OLS) regression line (dashed line) for two Ontario lakes and their corresponding rank-frequency plots (C–D), which gives the rank of body mass (μg), on a $\log_2$ axis, and the number of values ≥ mass fitted with a power law using the maximum likelihood estimate of the truncated Pareto exponent (dotted line).

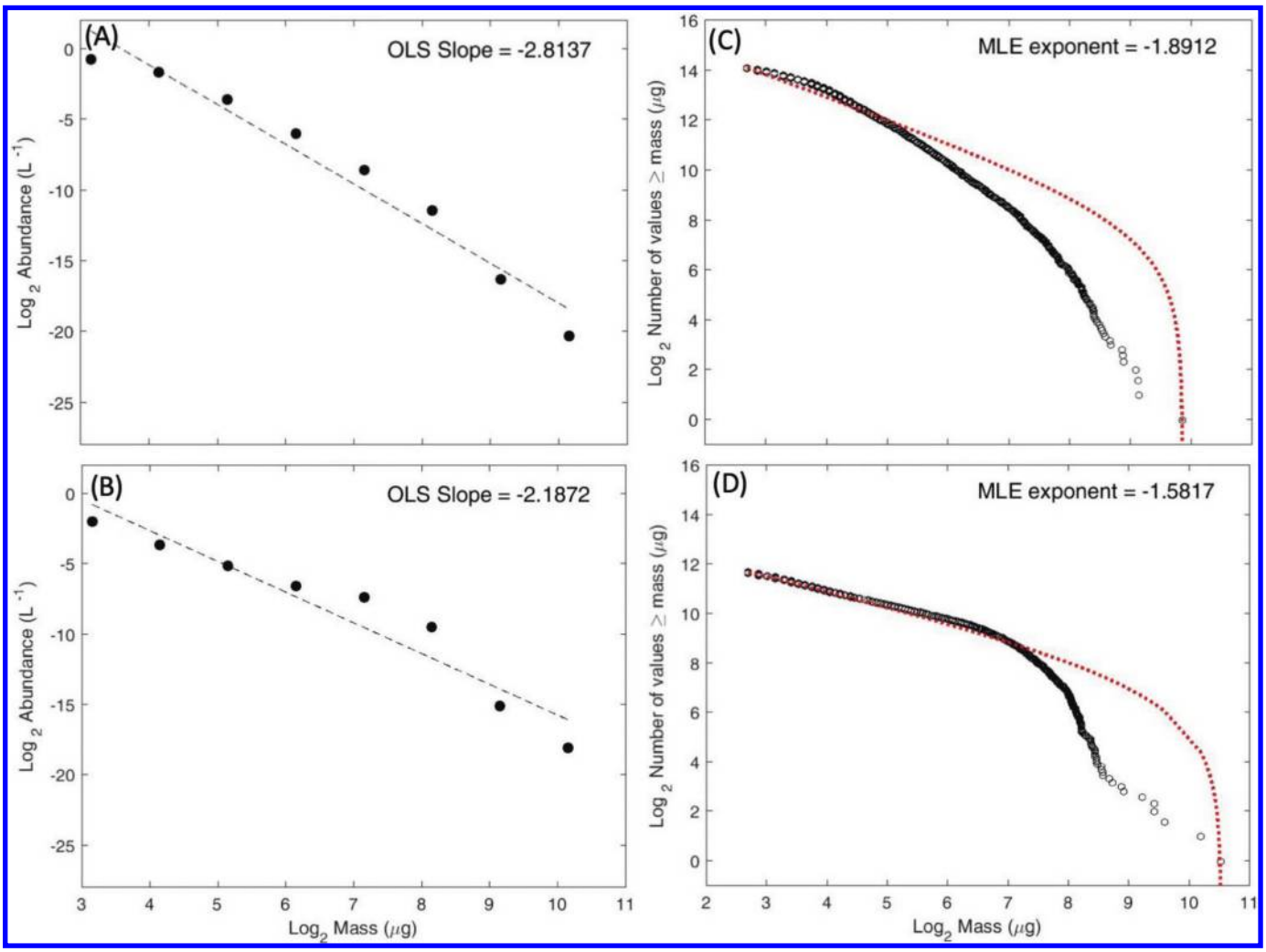

Fig. A2. Mean ± standard error of the seasonal pattern in the height (A) and OLS slope (B) of the zooplankton NASS averaged across years and lakes (n = 278 to 327 for each month).

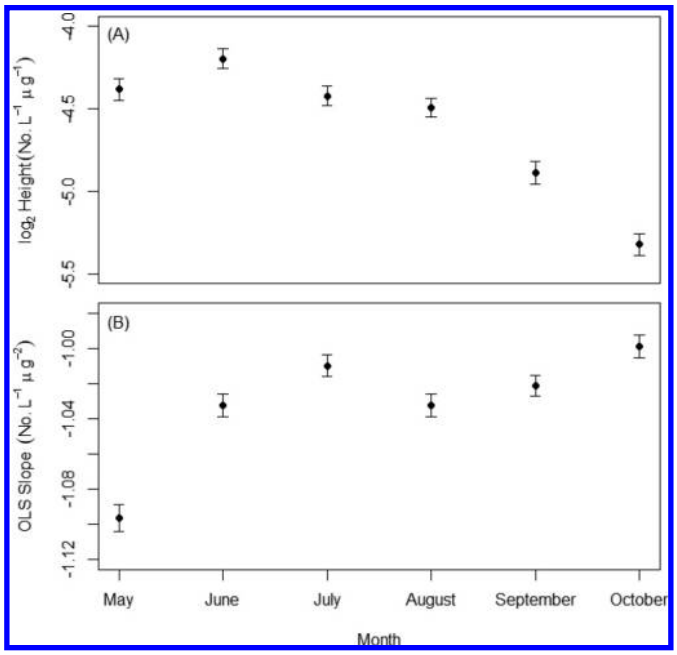

Table A1. List of candidate random, fixed, and mixed effects models used in model selection for the first two analyses.

Model No.	Model expression
Random effects models	
R1	$Y_m = B_0 + b_{0m} + e_m$
R2	$Y_y = B_0 + b_{0y} + e_y$
R3	$Y_l = B_0 + b_{0l} + e_l$
R4	$Y_{my} = B_0 + b_{0m} + b_{0y} + e_{my}$
R5	$Y_{yl} = B_0 + b_{0y} + b_{0l} + e_{yl}$
R6	$Y_{ml} = B_0 + b_{0m} + b_{0l} + e_{ml}$
R7	$Y_{myl} = B_0 + b_{0m} + b_{0y} + b_{0l} + e_{myl}$
R8	$Y_{yl} = B_0 + b_{0l} + b_{0y(l)} + e_{yl}$
R9	$Y_{ml} = B_0 + b_{0l} + b_{0m(l)} + e_{ml}$
R10	$Y_{my} = B_0 + b_{0y} + b_{0m(y)} + e_{my}$
R11	$Y_{myl} = B_0 + b_{0y} + b_{0l} + b_{0m(y)} + e_{myl}$
R12	$Y_{myl} = B_0 + b_{0m} + b_{0l} + b_{0y(l)} + e_{myl}$
R13	$Y_{myl} = B_0 + b_{0y} + b_{0l} + b_{0m(l)} + e_{myl}$
R14	$Y_{myl} = B_0 + b_{0l} + b_{0y(l)} + b_{0m(y(l))} + e_{myl}$
R15	$Y_{ml} = B_0 + b_{0m} + b_{0l} + b_{0ml} + e_{ml}$
R16	$Y_{my} = B_0 + b_{0m} + b_{0y} + b_{0my} + e_{my}$
R17	$Y_{yl} = B_0 + b_{0y} + b_{0l} + b_{0Yl} + e_{yl}$
R18	$Y_{myl} = B_0 + b_{0m} + b_{0y} + b_{0l} + b_{0my} + b_{0ml} + b_{0yl} + e_{myl}$
R19	$Y_{myl} = B_0 + b_{0m} + b_{0y} + b_{0l} + b_{0my} + b_{0ml} + b_{0Yl} + b_{0myl} + e_{myl}$
Fixed and mixed effects models	
M1	$Y_m = B_0 + B_{1m} + e_m$
M2	$Y_{my} = B_0 + B_{1m} + b_{0y} + e_{my}$
M3	$Y_{ml} = B_0 + B_{1m} + b_{0l} + e_{ml}$
M4	$Y_{myl} = B_0 + B_{1m} + b_{0y} + b_{0l} + e_{myl}$
M5	$Y_{myl} = B_0 + B_{1m} + b_{0y} + b_{0l} + b_{1l} + e_{myl}$
M6	$Y_{ml} = B_0 + B_{1m} + b_{0l} + b_{1l} + e_{ml}$
M7	$Y_{myl} = B_0 + B_{1m} + b_{0y(l)} + e_{myl}$
M8	$Y_{myl} = B_0 + B_{1m} + b_{0y(l)} + b_{0l} + b_{1l} + e_m$
M9	$Y_{myl} = B_0 + B_{1m} + b_{0y(l)} + b_{0l} + e_{myl}$
M10	$Y_{myl} = B_0 + B_{1m} + b_{0y} + b_{0l} + b_{1y} + e_{myl}$
M11	$Y_{myl} = B_0 + B_{1m} + b_{0y} + b_{0l} + b_{1y} + b_{1l} + e_{myl}$
M12	$Y_{myl} = B_0 + B_{1m} + b_{0y} + b_{0l} + b_{1y} + b_{1l} + b_{0Yl} + b_{1Yl} + e_{myl}$
M13	$Y_{my} = B_0 + B_{1m} + b_{0y} + b_{1y} + e_{my}$
M14	$Y_{myl} = B_0 + B_{1m} + b_{0y(l)} + b_{0l} + b_{1y(l)} + b_{1l} + e_{myl}$
M15	$Y_{myl} = B_0 + B_{1m} + b_{0y(l)} + b_{0l} + b1_{y(l)} + e_{myl}$

Note: Fixed and random effects in the models are identified by "B" and "b", respectively. b_{0y} indicates a random effect on the intercept (B_0), while b_1 indicates a random effect on the slope (B_1). Bold model numbers identify the best random (R) and mixed (M) effects models.

Table A2. Description of variables specified in all candidate random effects models.

Notation	Name	Description
Y_{myl}	Dependent variable	In analyses of the "height" of the normalized abundance size spectrum (NASS), this is the height estimated at size bin eight for each month (m), year (y), and lake (l) combination; in analyses of the slope of the NASS, this is the OLS slope estimated for each month, year, and lake combination.
B_0	Model intercept	In random effects analyses of NASS height, this is the grand mean of height across months, years, and lakes; in random effects analyses of NASS OLS slope, this is the grand mean of OLS slope across months, years, and lakes.
b_{0m}	Independent random month effect	Deviation from the grand mean for the mth month, where $b_{0m} \sim N(0, \sigma^2_m)$. A large σ^2_m implies that most of the variance in the NASS parameters is seasonal in origin. When expressed as the total variance explained by the month component (i.e., intraclass correlation coefficient (ICC) for month), it estimates the synchrony across lakes of seasonal fluctuations in the NASS parameters. This is referred to as a "global" effect because it is consistent across lakes.
b_{0y}	Independent random year effect	Deviation from the grand mean for the yth year, where $b_{0y} \sim N(0, \sigma^2_y)$. This is the temporal variance component, σ^2_y. When expressed as the total variance explained by the year component (i.e., ICC for year), it estimates the synchrony across lakes of yearly fluctuations in the NASS parameters. This is also referred to as a "global" effect, as it represents the among-year variance component consistent across lakes.
b_{0l}	Independent random lake effect	Deviation from the grand mean for the lth lake, where $b_{0l} \sim N(0, \sigma^2_l)$. This is the spatial variance component, σ^2_l, which estimates the amount of variance among lakes. This component would be best related to limnological characteristics of the lakes.
$b_{0m(y)}$	Nested random effect of month within year	Deviation from the grand mean for the mth month nested within the yth year after the effect of year has been accounted for independently, where $b_{0m(y)} \sim N(0, \sigma^2_{m(y)})$. $\sigma^2_{m(y)}$ estimates the amount of variance among months within years, and a large $\sigma^2_{m(y)}$ implies that there are large month-to-month fluctuations in the dependent variable within the same year. This nested structure means that there is no independent effect of month. The effect of month can only be interpreted within a given level of year.
$b_{0(l)}$	Nested random effect of year within lake	Deviation from the grand mean for the yth year nested within the lth lake after the effect of lake has been accounted for independently, where $b_{0y(l)} \sim N(0, \sigma^2_{y(l)})$. $\sigma^2_{y(l)}$ estimates the amount of variance among years within the same lake, and a large $\sigma^2_{y(l)}$ suggests that there are large year-to-year fluctuations in the dependent variable within a lake. This nested structure means that there is no independent effect of year. The effect of year can only be interpreted within a specific level of lake.
$b_{0m(l)}$	Nested random effect of month within lake	Deviation from the grand mean for the mth month nested within the lth lake after the effect of lake has been accounted for independently, where $b_{0m(l)} \sim N(0, \sigma^2_{m(l)})$. This nested structure implies that there is no global seasonal effect. Instead, the seasonal effect is specific to each lake. A large $\sigma^2_{m(l)}$ suggests that there are large month-to-month fluctuations in the dependent variable within a lake.
$b_{0m(y(l))}$	Nested random effect of month within year within lake	Deviation from the grand mean for the mth month within the yth year nested within the lth lake after the independent effect of lake and the nested effect of year within lake have been accounted, where $b_{0m(y(l))} \sim N(0, \sigma^2_{m(y(l))})$. A large $\sigma^2_{m(y(l))}$ indicates that there are large month-to-month fluctuations in the dependent variable within the same year for a given lake.
b_{0ml}	Random effect of the interaction between month and lake	Deviation from the grand mean for the mth month and the lth lake after these effects have been accounted for independently, where $b_{0ml} \sim N(0, \sigma^2_{ml})$. σ^2_{ml} estimates the additional variance due to the dependency between month and lake. A large σ^2_{ml} could arise if all or most of the lakes exhibit asynchrony in their seasonal pattern of variation.
b_{0my}	Random effect of the interaction between month and year	Deviation from the grand mean for the mth month and the yth year after these effects have been accounted for independently, where $b_{0my} \sim N(0, \sigma^2_{my})$. σ^2_{my} estimates the additional variance due to the dependency between month and year. A large σ^2_{my} could arise if all or most years exhibit asynchrony in their seasonal pattern of variation.
b_{0yl}	Random effect of the interaction between year and lake	Deviation from the grand mean for the yth year and the lth lake after these effects have been accounted for independently, where $b_{0yl} \sim N(0, \sigma^2_{yl})$. σ^2_{yl} estimates the additional variance due to the dependency between year and lake. A large σ^2_{yl} could arise if all or most lakes experience asynchrony in their year-to-year pattern of variation.
b_{0myl}	Random effect of the interaction among month, year, and lake	Deviation from the grand mean for the mth month, yth year, and the lth lake after the independent effects and the two-way interaction effects have been accounted for, where $b_{0myl} \sim N(0, \sigma^2_{myl})$ and σ^2_{myl} estimates the remaining variance associated with month, year, and lake. A large σ^2_{myl} could arise if seasonal fluctuations are lake-specific and differ from year to year.
e_{myk}	Residual random error	Describes how the OLS slope or the height observed for month m, year y, and lake l differs from that predicted by the model, and $e_{myl} \sim N(0, \sigma^2)$, where σ^2 is the residual variance component.

Note: The residual term in all models represents the deviation of the height or OLS slope observed for month m, year y, and lake l from that predicted by the model, where $e_{myl} \sim N(0, \sigma^2_e)$. All random effects and residual error terms are point estimates from a vector of normally distributed values with a mean of zero and variances estimated by the model (Hansen et al. 2015).

Table A3. Description of variables specified in all candidate mixed effects models.

Notation	Name	Description
Y_{myl}	Dependent variable	In analyses of the "height" of the normalized abundance size spectrum (NASS), this is the height estimated at size bin eight for each month, year, and lake combination; in analyses of the slope of the NASS, this is the OLS slope estimated for each month, year, and lake combination.
B_0	Model intercept	In mixed effects analyses of NASS height, this is the mean height at size bin eight in July averaged across all L lakes and Y years; in mixed effects analyses of NASS OLS slope, this is the mean OLS slope in July averaged across all L lakes and Y years.
B_1	Model slope	In mixed effects analyses of NASS height, this is average linear rate of change in height over the season for all Y years and L lakes; in mixed effects analyses of NASS OLS slope, this is average linear rate of change in OLS slope over the season for all Y years and L lakes. A significant fixed effect suggests that there is synchrony among lakes in the seasonal pattern of the NASS height or the NASS OLS slope (i.e., a "global" seasonal pattern).
b_{0y} and b_{1y}	Independent random year effect on the model intercept and model slope	A random effect in a mixed effects model can have an effect on both the model intercept (i.e., B_0) and the model slope (i.e., B_1) (i.e., the fixed effects). b_{0y} is the random year effect on the model intercept representing the deviation from the mean response in July for the yth year, and b_{1y} is the random year effect on the model slope representing the deviation from the mean seasonal linear rate of change in the response for the yth year, where $b_{0y} \sim N(0, \sigma^2_{0y})$ and $b_{1y} \sim N(0, \sigma^2_{1y})$. A large σ^2_{0y} could arise if there is synchrony across lakes in the yearly fluctuations of the model intercept (i.e., mean NASS height or NASS OLS slope in July), while a large σ^2_{1y} could arise if there is synchrony across lakes in the yearly fluctuations of the model slope (i.e., linear rate of change in the NASS height or the NASS OLS slope over the season). This would suggest that variability in the model intercept and model slope is driven by annual-scale factors.
b_{0l} and b_{1l}	Independent random lake effect on the model intercept and model slope	b_{0l} is the random lake effect on the model intercept (i.e., B_0) representing the deviation from the mean response in July for the lth lake, and b_{1l} is the random lake effect on the model slope (i.e., B_1) representing the deviation from the mean seasonal linear rate of change in the response for the lth lake, where $b_{0l} \sim N(0, \sigma^2_{0l})$ and $b_{1l} \sim N(0, \sigma^2_{1l})$. A large σ^2_{0l} implies that there is a strong lake-specific component influencing the model intercept (i.e., mean NASS height or NASS OLS slope in July), while a large σ^2_{1l} means that there is a strong lake-specific component influencing the model slope (i.e., linear rate of change in the height or the OLS slope over the season).
b_{0yl} and b_{1yl}	Random effect of the interaction between year and lake on the model intercept and model slope	b_{0yl} and b_{1yl} are the random effects of the interaction between the yth year and the lth lake on the model intercept (i.e., B_0) and model slope (i.e., B_1), respectively, where $b_{0yl} \sim N(0, \sigma^2_{0yl})$ and $b_{1yl} \sim N(0, \sigma^2_{1yl})$. A large σ^2_{0yl} could arise if there is asynchrony across lakes in the year-to-year fluctuations of the model intercept (i.e., mean NASS height or NASS OLS slope in July), while a large σ^2_{1yl} could arise if there is asynchrony across lakes in the year-to-year fluctuations of the model slope (i.e., linear rate of change in the NASS height or the NASS OLS slope over the season). This would suggest that there is little predictability in the seasonal patterns of the size spectrum.
$b_{0y(l)}$ and $b_{1y(l)}$	Nested random effect of year within lake on the model intercept and model slope	$b_{0y(l)}$ is the random year(lake) effect on the model intercept (i.e., B_0) representing the deviation from the mean response in July for the yth year nested within the lth lake, and $b_{1y(l)}$ is the random year(lake) effect on the model slope (i.e., B_1) representing the deviation from the mean seasonal linear rate of change in the response for the yth year nested within the lth lake, where $b_{0y(l)} \sim N(0, \sigma^2_{0y(l)})$ and $b_{1y(l)} \sim N(0, \sigma^2_{1y(l)})$. $\sigma^2_{0y(l)}$ estimates the amount of variance in the mean NASS height or NASS OLS slope in July among years within the same lake, and $\sigma^2_{1y(l)}$ estimates the amount of variance in the seasonal linear rate of change in NASS height or NASS OLS slope among years within the same lake. Large $\sigma^2_{0y(l)}$ could arise if there is asynchrony in the year-to-year fluctuations of the model intercept (i.e., mean NASS height or NASS OLS slope in July) within a lake, and a large $\sigma^2_{1y(l)}$ could arise if there is asynchrony in the year-to-year fluctuations of the model slope (i.e., linear rate of change in the NASS height or the NASS OLS slope over the season) within a lake.
e_{myl}	Random residual error	Describes how the observations of NASS height or NASS OLS slope across months differ from that which is predicted by the model for month m, year y, and lake l.

Note: Details as in Table A2.

Table A4. Results of random effects model selection using the minimum corrected Akaike information criterion (AIC_c).

Model	df	AIC_c	$\Delta_i(AIC_c)$	Akaike weight	R^2_C (%)
Height of the NASS					
R1	3	5659.1	1110.0	0.0	12.0
R2	3	5735.5	1186.4	0.0	8.6
R3	3	5254.8	705.7	0.0	32.6
R4	4	5542.6	993.6	0.0	21.2
R5	4	5100.4	551.4	0.0	40.5
R6	4	5011.8	462.8	0.0	42.9
R7	5	4813.8	264.7	0.0	51.1
R8	4	5053.8	504.7	0.0	48.1
R9	4	5015.2	466.2	0.0	43.1
R10	4	5644.5	1095.4	0.0	20.9
R11	5	4877.3	328.3	0.0	54.3
R12	5	4727.9	178.9	0.0	59.0
R13	5	4805.8	256.7	0.0	51.8
R14	5	4982.1	433.0	0.0	64.8
R15	5	4985.0	435.9	0.0	44.2
R16	5	5540.1	991.1	0.0	23.1
R17	5	5013.7	464.7	0.0	48.4
R18	**8**	**4549.1**	**0.0**	**0.7**	**66.6**
R19	**9**	**4551.0**	**1.9**	**0.3**	**67.0**
OLS slope of the NASS					
R1	3	−2703.0	226.7	0.0	7.7
R2	3	−2686.2	243.5	0.0	7.5
R3	3	−2613.6	316.0	0.0	1.4
R4	4	−2785.5	144.2	0.0	14.1
R5	4	−2701.8	227.9	0.0	9.4
R6	4	−2715.1	214.6	0.0	9.2
R7	5	−2802.5	127.2	0.0	15.9
R8	4	−2739.6	190.1	0.0	18.1
R9	4	−2710.8	218.9	0.0	10.5
R10	4	−2736.0	193.6	0.0	15.4
R11	5	−2754.4	175.3	0.0	17.5
R12	5	−2853.9	75.8	0.0	25.1
R13	5	−2803.3	126.4	0.0	17.6
R14	5	−2778.1	151.6	0.0	39.1
R15	5	−2731.8	197.9	0.0	11.8
R16	5	−2792.6	137.1	0.0	16.8
R17	5	−2760.7	169.0	0.0	18.6
R18	8	−2920.8	8.9	0.0	32.8
R19	**9**	**−2929.7**	**0.0**	**1.0**	41.4

Note: A total of 19 random intercept models (R1–R19) were fit using either the $\log_2$ height (no.·L^{-1}·μg^{-1}) or the OLS slope (no.·L^{-1}·μg^{-2}) of the NASS as the response variable. The $\Delta_i(AIC_c)$ was calculated as the minimum AIC_c value of the 19 models subtracted from each models AIC_c value. Akaike weights represent the normalized relative likelihood of a model, and the model fits were assessed using the conditional coefficient of determination (R^2_C). Best models are those with $\Delta_i(AIC_c) < 2$ and are shown in bold.

Table A5. Results of mixed effects model selection using the minimum corrected Akaike information criterion (AIC_c).

Model	df	AIC_c	$\Delta_i(AIC_c)$	Akaike weight	R^2_M	R^2_C
Height of the NASS						
M1	3	5687.3	1027.3	0	7.8	7.8
M2	4	5579.9	919.9	0	7.8	16.6
M3	4	5056.2	396.2	0	7.1	39.7
M4	5	4873.8	213.8	0	7.2	47.8
M5	7	4866.6	206.6	0	5.7	55.8
M6	6	5051.9	391.9	0	5.7	48.7
M7	4	4965.2	305.2	0	7.4	53.5
M8	7	4785.1	125.1	0	5.6	62.4
M9	5	4795.8	135.8	0	7.1	55.8
M10	7	4818.4	158.4	0	6.8	53.1
M11	9	4808.4	148.4	0	5.4	60.2
M12	**12**	**4660.0**	**0.0**	**1**	**5.1**	**69.4**
M13	6	5558.4	898.4	0	7.5	22.9
M14	9	4736.3	76.3	0	5.1	69.0
M15	7	4738.0	78.0	0	6.1	64.0
OLS slope of the NASS						
M1	3	−2660.7	185.3	0	3.8	3.8
M2	4	−2744.3	101.7	0	3.5	10.8
M3	4	−2672.0	174.0	0	3.7	5.2
M4	5	−2760.5	85.5	0	3.5	12.6
M5	7	−2772.4	73.5	0	3.9	15.9
M6	6	−2681.3	164.7	0	4.1	8.3
M7	4	−2803.6	42.3	0	3.4	21.3
M8	7	−2817.9	28.1	0	3.9	23.4
M9	5	−2804.2	41.8	0	3.4	21.4
M10	7	−2764.8	81.2	0	3.6	13.0
M11	9	−2775.8	70.1	0	3.9	16.3
M12	**12**	**−2846.0**	**0.0**	**1**	**3.6**	**31.5**
M13	6	−2748.4	97.6	0	3.6	11.1
M14	9	−2822.0	24.0	0	3.6	31.2
M15	7	−2813.2	32.7	0	3.4	29.9

Note: One fixed effect model (M1) and 14 mixed effect models (M2–M15) were fit using either the $\log_2$ height (no.·L^{-1}·μg^{-1}) or the OLS slope (no.·L^{-1}·μg^{-2}) of the NASS as the response variable. Models M1–M15 were fit with restricted maximum likelihood (REML) and compared to determine the random structure of the "best" model. Goodness of fit for the fixed and total model components were assessed using the marginal and conditional coefficient of determination, respectively (R^2_M and R^2_C). Details as in Table A4.

Table A6. Mean estimates ± standard error (SE) of intercept and linear rate of change (Lin.Δ) from the mixed effects model M12 for the height and the OLS slope of the NASS (note the $\log_2$ scale for the intercept of the model containing the response height).

	Estimate	SE	df	*t* value	*p* value
Height					
Intercept	−4.511	0.249	7.7	−18.1	<0.0001
Lin.Δ	−0.179	0.033	17.6	−5.4	<0.0001
OLS slope					
Intercept	−1.036	0.008	18.8	−131.7	<0.0001
Lin.Δ	0.014	0.004	8.3	4.0	0.0035

Note: Significance tests were one-sample *t* tests on each fixed effect to determine whether the coefficient was significantly different from zero.

Table A7. Mean estimate ± standard error (SE) of the difference between the observed height or the OLS slope of the NASS and the seasonal mean value for each lake.

Coefficient	Estimate	SE	*t* value	*p* value	Relative to seasonal mean
Height of the NASS					
May	0.088	0.055	1.6	0.1109	=
June	0.286	0.054	5.3	<0.0001	>
July	0.094	0.054	1.7	0.0834	=
August	0.109	0.038	2.9	0.0043	>
September	−0.387	0.055	−7.1	<0.0001	<
October	−0.772	0.056	−13.8	<0.0001	<
OLS slope of the NASS					
May	−0.060	0.008	−7.7	<0.0001	<
June	−0.001	0.008	−0.1	0.945	=
July	0.022	0.008	2.9	0.004	>
August	−0.002	0.005	−0.3	0.7462	=
September	0.011	0.008	1.5	0.1407	>
October	0.029	0.008	3.6	0.0003	>

Note: For each lake and year, we calculated the seasonal mean $\log_2$ height and OLS slope and subtracted these values from the observed value of $\log_2$ height and OLS slope. Generalized least squares models using maximum likelihood estimation were fit to these data to estimate the fixed effects (i.e., the mean difference). One-sample *t* tests on the mean difference were used to determine whether the mean difference for a month was significantly different from zero. Symbols display the relationship of the height or OLS slope value relative to the seasonal mean for a lake (=, equal to seasonal mean; <, less than season mean; >, greater than seasonal mean).